

Montana Tech Library

Digital Commons @ Montana Tech

Graduate Theses & Non-Theses

Student Scholarship

Spring 5-4-2024

Application of Biochar / Bentonite Based Admixtures in Reinforced Concrete for Corrosion Prevention

Jacob Fleury

Follow this and additional works at: https://digitalcommons.mtech.edu/grad_rsch



Part of the [Mechanical Engineering Commons](#)

Application of Biochar / Bentonite Based Admixtures in Reinforced Concrete for
Corrosion Prevention

by
Jacob B. Fleury

A thesis submitted in partial fulfillment of the
requirements for the degree of

General Engineering – Mechanical Option

Montana Tech

2024



Abstract

Reinforced concrete systems are in many sectors of infrastructure. Due to a combination of elevated compressive strength from the cement and aggregates and tensile strength from the reinforcing steel, reinforced systems are favorable in construction applications where high strength is desired. However, while reinforced concrete is in service, it can be introduced to contaminants that cause corrosion. Contaminants can leach through the porous matrix of the concrete structure and influence initiation of corrosion products on reinforcement. Corrosion is the primary cause for advanced deterioration of concrete structures. Concrete deterioration has promoted research efforts for the protection of future systems. This research evaluates the suitability of corrosion resistance with the implementation of biochar and bentonite admixtures in concrete. Methods for determination of suitability include open circuit potential testing, force migration testing and strength testing on various admixture integrations. Each testing scenario ultimately indicates that the combination of biochar and bentonite negatively influences corrosion resistance and strength characteristics.

Keywords: Reinforced Concrete, Biochar, Bentonite, Open Circuit Potential, Forced Migration,

Dedication

This work is dedicated to my family. Without their love and support, this would not have been possible.

Acknowledgements

Special thanks are due to my advisor, Dr. Richard LaDouceur, for giving me an opportunity to enhance my engineering knowledge through additional coursework and research in Graduate School. Dr. LaDouceur has provided me with mentorship, encouragement, and inspiration during my time as a student. I hope I can match his enthusiasm for engineering as I begin my career. Appreciation is also due to my committee members Dr. Mario Caccia, and Prof. Scott Coguell. Dr. Caccia and Prof Coguell each offered different viewpoints throughout my research. Dr. Caccia gave an insight into the understanding of material science, while Prof. Coguell gave insight from industry experience. Special thanks are also due to Dr. Bret Robertson for sharing some of his knowledge about concrete systems. Acknowledgements should also be given to Administrative Assistant Julie Crowley for the assistance in ordering materials. Finally, I would like to extend my thanks to fellow CHAR Lab researchers for their collaboration efforts and comradery. Specifically: Max Triepke, Kelli Thomas, Joe Salerno, Amir Riahi, Zainab Nasrullah, Frank Agyemang.

Research was sponsored by the Combat Capabilities Development Command Army Research Laboratory and was accomplished under Cooperative Agreement Number W911NF-20-2-0163. The views and conclusions contained in this document are those of the authors and should not be interpreted as representing the official policies, either expressed or implied, of the Combat Capabilities Development Command Army Research Laboratory or the U.S. government.

Table of Contents

Abstract	II
Dedication	III
Acknowledgements	IV
List of Figures	VII
List of Tables	VIII
List of Equations	IX
1.0 Introduction	1
2.0 Background	2
2.1 Concrete Basics	2
2.1.1 Cement Production and Hydration	4
2.2 Concrete Corrosion	6
2.2.1 Carbonation	6
2.2.2 Chloride Attack	7
2.2.3 Concrete Corrosion Identification	10
2.3 Corrosion Mitigation Methods	13
2.3.1 Natural Corrosion Blockers	13
2.3.2 Engineered Corrosion Blockers	14
2.4 Biochar	17
2.5 Bentonite Clay	19
3.0 Methodology/Materials	20
3.1 Concrete Mix Design/Mixing	21
3.2 Open Circuit Potential Testing	27
3.3 Forced Migration Testing	30
3.3.1 Diffusion Cell Construction	35
3.4 Strength Testing	36
4.0 Results/Discussion	39
4.1 Mixing	39
4.2 Open Circuit Potential Test	40
4.3 Forced Migration Test	44

4.4	Strength Test and Density	54
5.0	Conclusion	57
5.1	Limitations	58
5.2	Recommendations	59
5.3	Future Work	59
6.0	Appendix	60
6.1	ACI 211 Design Tables	60
6.2	Mix Design Calculations	62
6.2.1	Mix 1 Design Calculations	62
6.2.2	Mix 2 Design Calculations	65
6.3	Open Circuit Potential Data	68
6.3.1	Electrical Potential Voltage for Samples in NaCl	68
6.3.2	Electrical Potential Voltage for Samples in Ca(OH)₂	69
6.3.3	Electrical Potential Voltage for Samples in Na₂SO₄	70
6.4	Forced Migration Calculations and Data	71
6.4.1	4 – 25:75	72
6.4.2	4 – 50:50	74
6.4.3	4 – 75:25	76
6.4.4	8 – 25:75	77
6.4.5	8 – 50:50	78
6.4.6	8 – 75:25	79
6.4.7	Control	81
6.5	Strength and Density Calculations and Data	82
6.5.1	28 Day Compressive Strength	82
6.5.2	28 Day Bending Strength	83
6.5.3	Density	84
7.0	Resources	85

List of Figures

Figure 1 - Water-Cement Ratios Effect on Porosity and Strength [6]	5
Figure 2 - Evolution of Carbonation Progression [9].....	7
Figure 3 – Table of Critical Pitting Potential Voltages of Different Metal and Alloys [8].....	9
Figure 4 - Schematic of Pitting and Rust Formation on Rebar in Concrete [10]	9
Figure 5 - Example of Rust Staining.....	11
Figure 6 - Example of Efflorescence Staining	11
Figure 7 - Example of Delamination and Exposed Rebar.....	12
Figure 8 - Example of Spalling	13
Figure 9 - Galvanic Series of Metals [8].....	15
Figure 10 - Zinc Puck Cathodic Protection [18]	16
Figure 11 - Biowaste Products for Production of Biochar	17
Figure 12 - Prolongation of Cement Hydration Upon Biochar Desorption of Water [22]	18
Figure 13 - Schematic of OCP Test [30].....	28
Figure 14 - Samples in Solution for Wet OCP Measurements	30
Figure 15 - 3D Solid Model of Diffusion Cell.....	31
Figure 16 - Internal Section View of 3D Solid Model.....	31
Figure 17 - Diffusion Cell Section and Details.....	32
Figure 18 - Conductivity vs Concentration Profile for NaCl.....	33
Figure 19 - Typical Diffusion Curve for Concrete.....	34
Figure 20 - Compressive Strength Test Frame	37
Figure 21 - 4-Pt Bending Strength Tests.....	38
Figure 22 - Example of Typical Salt Scaling on Na ₂ so ₄ Samples	40
Figure 23 - Reinforcement from Slabs in OCP Testing.....	42
Figure 24 - Potential vs Time for Samples in NaCl.....	42
Figure 25 - Potential vs Time for Samples in Ca(OH) ₂	43
Figure 26 - Potential vs Time for Sample in Na ₂ SO ₄	44
Figure 27 - Typical Rust Film Development and De-cementation of Exposure Surface	45
Figure 28 - Anolyte Concentration vs Time 4 - 25:75	46
Figure 29 - Anolyte Concentration vs Time 4 - 50:50.....	47
Figure 30 - Anolyte Concentration vs Time 4 - 75:25.....	48
Figure 31 - Anolyte Concentration vs Time 8 - 25:75.....	49
Figure 32 - Anolyte Concentration vs Time 8 - 50:50.....	50
Figure 33 - Anolyte Concentration vs Time 8 - 75:25.....	51
Figure 34 – Anolyte Concentration vs Time Control.....	52
Figure 35 - Diffusion Coefficient Batch Comparison.....	53
Figure 36 - Average 28 Day Compressive Strength	54
Figure 37 – 28 Day Bending Strength	56
Figure 38 - Average Density.....	57

List of Tables

Table 1 - Batch Design for Experimental Testing of Corrosion Resistance	20
Table 2 - Concrete Volume Required for Sample Creation.....	21
Table 3 - Absorption Capacity and Moisture Content for Aggregates Used in Mix Design	25
Table 4 – Mix Design for Mix 1 Samples.....	26
Table 5 - Mix Design for Mix 2 Samples	26
Table 6 - Corrosion Risk Severity Criterion	29
Table 7 - Molar Concentration and Conductivity for Profile Development	33
Table 8 - Constants for Calculation of Diffusion Coefficient.....	35
Table 9 - Mix 1 Actual Water Weight, Slump, and W:C.....	39
Table 10 - Mix 2 Actual Water Weight, Slump, and W:C.....	39
Table 11 - Flux, Diffusion Coefficient, and Initial Catholyte Concentration 4 - 25:75.....	46
Table 12 - Flux, Diffusion Coefficient, and Initial Catholyte Concentration 4 - 50:50.....	47
Table 13 - Flux, Diffusion Coefficient, and Initial Catholyte Concentration 4 - 75:25.....	48
Table 14 - Flux, Diffusion Coefficient, and Initial Catholyte Concentration 8 - 25:75.....	49
Table 15 - Flux, Diffusion Coefficient, and Initial Catholyte Concentration 8 - 50:50.....	50
Table 16 - Flux, Diffusion Coefficient, and Initial Catholyte Concentration 8 - 75:25.....	51
Table 17 - Flux, Diffusion Coefficient, Initial Catholyte Concentration Control.....	52
Table 18 - Average Flux, Diffusion Coefficient, and Initial Catholyte Concentration Batch Comparison	53
Table 19 – Average Peak Load and 28 Day Compressive Strength	55
Table 20 - Peak Load, Maximum Moment, And 28 Day Bending Strength.....	56
Table 21 - Weight and Density	57
Table 22 - Corrected Modification Factors for Fine Aggregate and Water Weight in Mix 1.....	58
Table 23 - Corrected Modification Factor for Fine Aggregate and Water Weight in Mix 2	58

List of Equations

Equation 1 - Cement and Water Reaction.....	4
Equation 2 - Carbonation Reaction 1.....	6
Equation 3 - Carbonation Reaction 2.....	6
Equation 4 - Water Weight Calculation.....	23
Equation 5 - Cement Weight Calculation.....	23
Equation 6 - Fine Aggregate Weight Calculation.....	23
Equation 7 - Component Volume Calculation.....	23
Equation 8 - Coarse Aggregate Volume Calculation.....	24
Equation 9 - Coarse Aggregate Weight Calculation.....	24
Equation 10 - Absorption Capacity Calculation.....	24
Equation 11 - Modified Aggregate Weight Calculation.....	25
Equation 12 - Modified Water Weight Calculation.....	25
Equation 13 - Anodic Half-Cell Reaction in Reference Electrodes.....	27
Equation 14 - Cathodic Half-Cell Reaction in Reference Electrodes.....	28
Equation 15 - Net Half-Cell Reactions for Reference Electrodes.....	28
Equation 16 - Nernst Equation for Net Half-Cell Reaction.....	28
Equation 17 - Molar Concentration Calculation.....	29
Equation 18 - Diffusion Coefficient Calculation.....	35
Equation 19 - Compressive Stress Calculation.....	37
Equation 20 - Maximum Moment for 4-Pt Bending.....	38
Equation 21 - Bending Stress Calculation.....	39

1.0 Introduction

Reinforced concrete is one of the most important building blocks of modern construction. Due to its high-strength capacity, it is used in many applications ranging from sidewalks to skyscrapers. Elevated available strength occurs due to the hardenability of cement upon curing, the natural compressive resistance of aggregates implemented in mixing, and the tensile strength of steel reinforcement. A disadvantage of concrete is that it has a porous microstructure. As concrete structures age, harmful contaminants can diffuse through the interconnected pores and degrade the steel reinforcement. Corrosion is problematic because it is the primary influence of concrete deterioration. The combination of deterioration and the fact that many concrete structures are approaching the end of their useful serviceability has led to research efforts for the protection of future systems. Research detailed in this paper looks at the suitability of biochar and bentonite clay additions for corrosion mitigation in reinforced concrete systems. Biochar is a carbon rich material which is a primary byproduct of thermal decomposition of biomaterials and biowastes. It has high adsorptive capacities which can attract harmful contaminants. Bentonite clay is a siliceous material which is predominantly made of calcium montmorillonite. Due to water adsorption, bentonite clay can swell and act as a pore filler or sealant. It is widely used to seal natural ponds and well casings to limit potential leaking. To evaluate the suitability of biochar and bentonite clay addition for corrosion prevention, several mixing ratios were designed for sample creation of material test specimens. Testing methods included strength evaluation to see the influence each ratio had on strength capacity, open circuit potential measurements to assess risk of corrosion with time, and forced migration testing to determine rate of ingress of harmful contaminants.

2.0 Background

2.1 Concrete Basics

Concrete is an engineered composite material that is readily used throughout the world's infrastructure. The key components of the composite include aggregates and a binding matrix to hold the aggregates together. Typical aggregates include sand, gravel, or crushed rock. In extreme cases, like nuclear applications, steel bearings can also be used. Binding matrices, or pastes, contain water and cementitious materials that interact with each other upon mixing [1]. Together, both elements provide strength which can resist different force applications when in service. Concrete strength development is largely attributed to the curing reaction between water and cement. Upon curing, the paste becomes a strong, rigid, hardened material. A hardened cement matrix on its own could provide ample desired compressive strength, but aggregates are implemented to reduce costs, improve production rates, and scale down emissions all while maintaining strength levels [2]. Maintained compressive strength can be achieved from two aggregate mechanisms, grain interlocking and natural compressive strength. Grain interlocking is achieved when a wide distribution of particle sizes is implemented in a mix and particles can compact against each other. Interlocking particles enable crack deflection in the concrete matrix. Aggregate's main role is to reduce the volume of required cement for construction products; however, their use can influence other parameters like workability, curing, and total costs. The use of aggregates also provides a clear definition between cement and concrete, which are terms that are often used synonymously outside of the concrete industry. Cement is one component of concrete, while cement coupled with aggregates is concrete [3].

Although concrete is advantageous in resisting compressive loading applications, it is weak under tensile stress. Available strength against tensile loads is approximately 10% of maximum available compressive strength [4]. If concrete is induced to tensile loading, fast brittle fracture

can occur. Rapid fracture could be catastrophic for public infrastructure. Historically, this issue has been mitigated by designing structures that do not experience tensile stress. Examples include domed or arched architecture. The modern solution against tension weak concrete is placement of steel reinforcement. Steel exhibits ductile behavior when yielded which allows for deflection of the concrete to occur without development of rapid tensile fracture. Typical steel reinforcement is made in circular bar form, otherwise known as rebar (reinforcement bar) and carries ribs which interlock with concrete to provide necessary strength. The ribs increase friction at the rebar-concrete interface and prevent slipping.

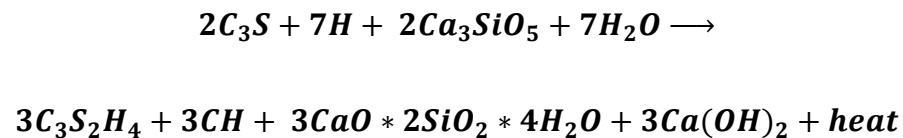
Materials other than aggregates, cement, and reinforcement that can be implemented in concrete are called admixtures. Admixtures are often added to mixes to enhance specific desirable properties. Properties that can be influenced are workability, curing time, corrosion inhibition, reduced weight, and coloring. Workable concrete is desirable because it ensures sufficient consolidation around reinforcement can be achieved. Admixtures that influence workability include water reducers or plasticizers which make concrete less viscous and able to flow easier. Dampening of viscosity occurs due to lowering of water surface tension and enhanced wetting action. Sodium lignosulphonate is an example of a water reducer. Curing time can either be retarded or accelerated based on environmental conditions during pouring. Retarding admixtures are used in hot weather where heat causes faster curing and poor workability. Retarders slow the growth of hydration by reducing the rate of which water reaches cement. An example of a retarder is sugar. Accelerating admixtures are used in cold weather where there is concern of ice formation in the water of the mix. Accelerating admixtures work by decreasing the freezing point of the water within concrete so frost formation can be limited. An example would be calcium chloride. Corrosion inhibiting admixtures are added to protect the steel reinforcement. Typical

inhibitors either adsorb contaminants or are film formers to protect steel. Concrete weight reduction can be fulfilled by introducing air into the mix. Air allows more porosity pockets to form which reduces the volume of required concrete. Coloring of concrete is a detail that is associated with finished product and can be achieved with dyes and pigments [5].

2.1.1 Cement Production and Hydration

Cementitious materials are derived from limestone and clay deposits. After harvest, these materials are crushed and mixed in a kiln. Heat from the kiln allows reactions to occur between the materials which creates clinker, a cluster of rounded cementitious beads. Clinker is then mixed with gypsum and ground down to a fine powder producing Portland cement [1]. To manufacture more cement, more mining is required, more material shipping is needed, increased gas consumptions occur, and wear and tear happens faster on machinery. All factors heighten cost, increase lead times, and produce emissions [6].

Portland cement contains calcium silicates, calcium aluminates, and calcium aluminum ferrites. When water is added to cement, calcium and hydroxide ions form and heat is generated.



Equation 1 - Cement and Water Reaction

Due to the presence of hydroxide ions, the material quickly becomes basic with a pH around 12. At this level, concrete can be caustic in handling causing dry and irritable skin. As a mix becomes saturated with ions, calcium hydroxides and different calcium silicates or calcium aluminates crystallize and allow nucleation to occur. Nucleation can either occur at the exterior boundaries near the form work, at the cement-aggregate interface, or at the cement-rebar interface. At each interface, solidification can occur from heterogeneous nucleation of hardened

cement. Heterogenous nucleation can occur because the energy to change from the liquid phase of hydrated cement to the solid phase of hardened cement is minimized [7]. With continued curing, hydroxide and silicate layers thicken and reduce water pockets until nominal design strength is achieved. Nominal design strength occurs approximately twenty-eight days after initial pouring. Strength can continue to develop after the twenty-eight-day mark but typically only changes in very small increments. Curing will progress if water and cement reactants are still present. Balancing the rate at which each reactant is used will optimize curing. Low water-cement ratios, approximately 1 water:2 cement, are desired for optimized curing and formation of small pore spaces. Really low ratios cause the water to be the limiting reagent which causes some calcium silicates to not be hydrated therefore full strength cannot be achieved. High water-cement ratios allow for cement to be the limiting reagent which causes excess water that make large pores and take away from area to resist force [1].

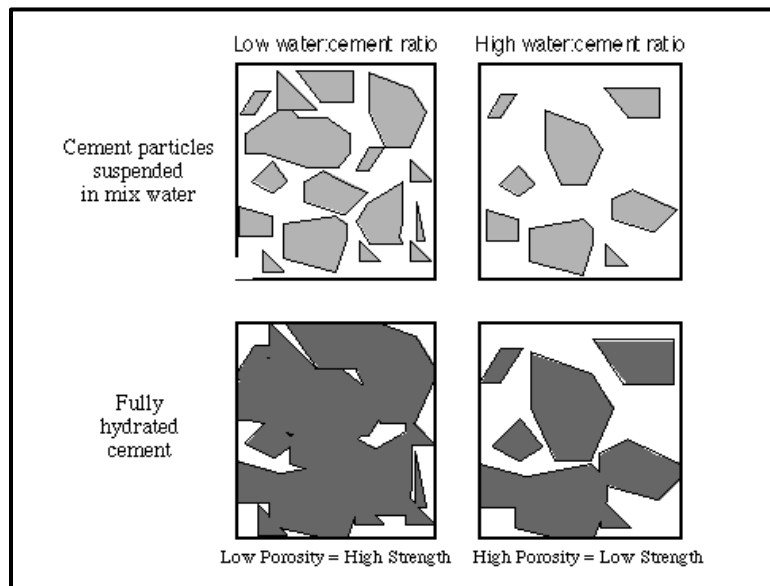


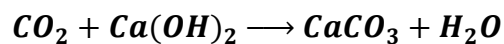
Figure 1 - Water-Cement Ratios Effect on Porosity and Strength [6]

2.2 Concrete Corrosion

Corrosion can be defined as the degradation of metal when exposed to harmful attack mechanisms. [8]. Based on this definition, concrete corrosion is an ambiguous term because concrete is not metal, rather it is comprised of a metal-based reinforcement which provides additional strength resistance. Corrosion that occurs within concrete only occurs on the reinforcement surface. Products of corrosion are the primary influence for advancement of concrete deterioration.

2.2.1 Carbonation

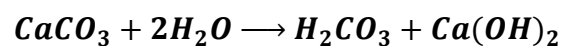
One attack mechanism that concrete endures is carbonation. Carbonation is the development of carbonates within a concrete matrix due to the reaction between carbon dioxide and calcium hydroxide.



Equation 2 - Carbonation Reaction 1

Carbon dioxide is introduced into concrete through a variety of mechanisms. Diffusion can occur due to changes in partial pressure from changing weather conditions or due to accumulation of man-made carbon dioxide. Exposure could also occur due to the development of acid rain.

Molecules can travel along pore networks that were created during concrete curing and react with the previously formed calcium hydroxide. Upon mixing, calcium hydroxide breaks down to calcium oxide and water. Carbon dioxide and calcium oxide produce carbonates. Carbonates can associate with excess water to form more calcium hydroxide and carbonic acid.



Equation 3 - Carbonation Reaction 2

Generation of carbonic acid can decrease the pH of concrete causing acidification, where pH is less than 7. Progression of acidification can deteriorate the passive film that is developed when concrete cures around steel reinforcement and allows faster corrosion to occur. Depassivation is undesirable because steel reinforcement is then unprotected and can further rust which could lead to compromised structural integrity of a concrete structure.

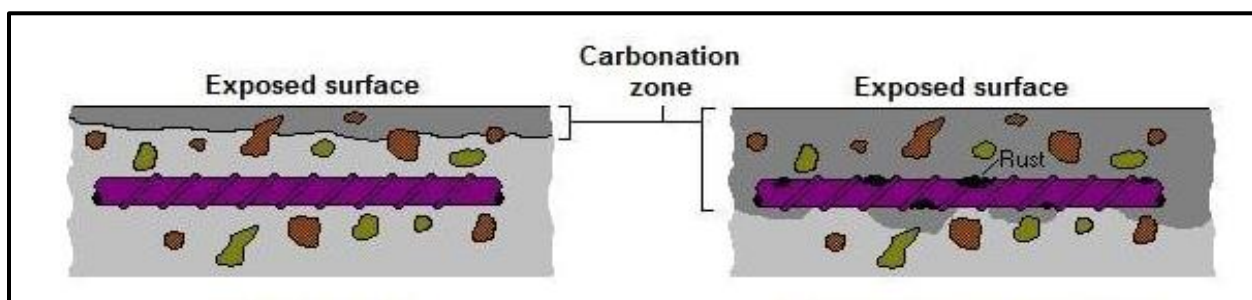


Figure 2 - Evolution of Carbonation Progression [9]

If acidification is shallow enough to not reach reinforcement, concrete can experience growth of strength due to the formation of new calcium hydroxide. Elevated early life strength from carbonation can ultimately lower concrete service life because the risk of depassivation is amplified after initial exposure [9]. Since concrete structures experience exposure to carbon dioxide throughout their entire serviceable life depassivation is more likely to occur in older structures. This is a concern because there are many aging structures approaching the end of their lives.

2.2.2 Chloride Attack

Chloride ion ingress is another harmful attack mechanism concrete experiences in its expected service life. Chloride attack is the most common salt attack to concrete, sulfate attack can also occur but that is a different process. Once introduced, ions diffuse through the porous matrix of the concrete and interact with the reinforcement causing corrosion. Mechanisms for integration

of chloride in concrete include capillary action and diffusion of saturated solutions. Exposure of chloride is due to both external and internal factors. External factors are those that are outside of the concrete system and can potentially infiltrate in. Examples include placement of concrete in oceanic seawater or brackish water, use of de-icing salts on transportation infrastructure, displaced wind-blown salt, or salt found within soil. Internal factors account for salts that can be pre-integrated within the concrete at the time of mixing. These include aggregates with infused trace amounts of salt, contaminated mixing water, or certain concrete admixtures [10].

Corrosion from chloride attack occurs due to pitting of the reinforcement surface. Pitting is a localized defect that disrupts the passive layer formed around reinforcement. Characterization of pitting is based on a metal's critical pitting potential voltage, E_{Pit} . Voltage, or electrical potential, is the electric force between positively and negatively charged ions. In corrosion processes, an electrode potential occurs when metals are in a solution of water and an interfacial film between the metal and the water produces the positive and negative charges. Metals measured with negative electrode potential are generally more reactive and favor oxidation corrosion. Metals measured with a positive electrode potential are more noble and favor reduction corrosion. The same process applies to reinforcement in concrete; however, the concrete matrix is assumed to be fully saturated in salt water. Critical pitting values are dependent on the type of metal and the concentration of salt in solution. As salt concentration increases critical pitting voltage decreases. Values above the critical voltage are more prone to pit development, values below are less prone. Typically metals that have more positive E_{Pit} are more resistant to pitting because they are more noble. Steels are susceptible because they have a low critical value in seawater [8].

Metal or alloy ^a	E_{pit} in V vs. SCE	Source
Zinc	-1.02	Alvarez and Galvele [94]
Aluminum	-0.70	Natishan et al. [95]
Al alloy 5656 (Al-5 Mg)	-0.68	Trzaskoma et al. [96]
Iron	-0.41	Strehblow and Titze [97], Alvarez and Galvele [98]
M-50 steel (Fe-4 Cr-5 Mo-1 V)	-0.23	Wang et al. [99]
Copper	-0.04	Thomas and Tiller [100]
Molybdenum	+0.055	Wang et al. [99]
Nickel	+0.08	Strehblow and Titze [97]
Chromium	+0.125	Wang et al. [99]
Zirconium	+0.22	Cragolino and Galvele [101]
304 stainless steel	+0.30	McCafferty and Moore [62]
316 stainless steel	+0.50	McCafferty and Moore [62]
Titanium	> +1.0 ^b	Dugdale and Cotton [102]

Figure 3 – Table of Critical Pitting Potential Voltages of Different Metal and Alloys [8]

Upon capillary action or diffusion of salt water into concrete, salt ions can penetrate the passive film developed around reinforcement. Ion penetration can occur because the passive film consists of a porous microstructure. As penetration evolves, vacancies developed between the metal and the film where local film thinning occurs. Eventually the film detaches from the metal and can crack from stresses in the concrete. When unprotected metal is exposed, pit growth occurs from acidification. Iron cations that are created from the exposed metal react with hydroxides to form rust.

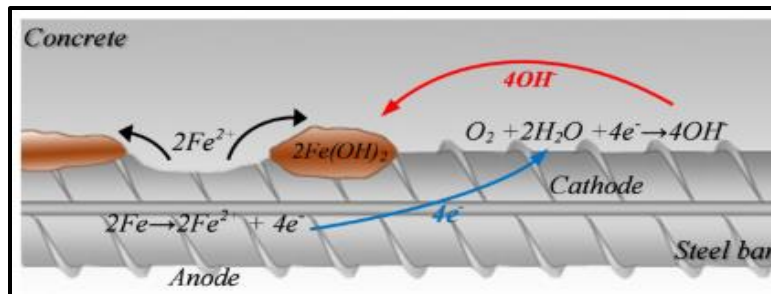


Figure 4 - Schematic of Pitting and Rust Formation on Rebar in Concrete [10]

2.2.3 Concrete Corrosion Identification

Concrete corrosion is problematic because it can progress unnoticed within structures. A large aspect for why overlooking occurs is because rebar systems cannot be seen directly, due to being placed within the concrete matrix. Another aspect for unobserved corrosion progression is time for degradation to occur. The evolution of corrosion is a slow process, typically years and decades in scale, so apparent structural changes, if any, can be minute. Major issues that arise without notice are rust formations and loss of area of steel. To monitor deterioration, most concrete structures follow regularly scheduled inspections by engineers or corrosion experts. Bridges on U.S. highway systems for example, are routinely checked every two years, where corrosion identification is one of the major aspects investigated [11]. When examined, inspectors look for identifying markers like rust staining, efflorescence staining, spalling, delaminations, cracking, and in extreme cases exposed rebar. Rust staining occurs as a red-orange discoloration on concrete surfaces. These stains form when oxidized material leaches outwards through the porous makeup of the concrete from the reinforcement to the surface exposed to the atmosphere. Efflorescence staining is white discoloration that occurs when excess moisture is present on the surface of the concrete and salt is left behind when dried.



Figure 5 - Example of Rust Staining



Figure 6 - Example of Efflorescence Staining

Spalls are sections of concrete that are broken into smaller pieces when multiple cracks diverge from reinforcement. Cracks form because rust can occupy more volume than parent metal. Increased volume from the corrosion product creates internal stress within the concrete matrix that requires fracture for relief. Delaminations are like spalls because they are formed by diverging cracks, however complete separation occurs between the rebar and concrete interface.

Delaminations often coincide with exposed rebar because of the interfacial separation. Exposed rebar is more susceptible to the effects of corrosion because there is no longer protection against the environment. Spalls only occur through the depth of the protective concrete cover but can progress into delaminations. Size and quantity of spalls and delaminations depends on the severity of the corrosion within the rebar system. These two identifying markers can be removed from the structure with minimal effort and can present a safety hazard for the public. When identified, rehabilitation efforts are prioritized to ensure public safety. In most cases, if any indicators are present under visual examination, corrosion has already developed [12].



Figure 7 - Example of Delamination and Exposed Rebar



Figure 8 - Example of Spalling

2.3 Corrosion Mitigation Methods

2.3.1 Natural Corrosion Blockers

Concrete is versatile because if designed and mixed properly it can possess numerous mechanisms that inhibit corrosion initiation on reinforcement. One mechanism is the ability to form the passive film at the concrete-reinforcement interface. Passivation can develop due to the alkaline environment that is produced upon cement hydration. Formation of the passive film limits the steel from reacting back to its thermodynamically stable state of active iron oxide. Since steel is a processed compound, large amounts of induced energy can destabilize the metal. Materials are thermodynamically stable when they are at minimized induced free energy [13]. Corrosion will still occur on passive films, but due to a small porous microstructure, rates are very slow [14]. Passive films are comprised of austenitic maghemite ($\gamma\text{-Fe}_2\text{O}_3$) while more active films are comprised of iron hydroxide ($\text{Fe}(\text{OH})_2$) [15]. Iron hydroxide has a larger porous microstructure which causes the larger volume occupation in concrete.

Pore structure of concrete influences permeability and electrical resistivity which are additional mechanisms that can inhibit corrosion initiation. If suitable water-cement ratios are utilized pore networks are small. Reduced pore size restricts permeability of contaminant infiltration. Small size pores also allow for high electrical resistivity. High electrical resistivity restrains the ability for changes in electrochemical energy. Changes in electrochemical energy cause changes in voltages which produce corrosion products [16]. In addition to pore structure, permeability can also be limited from aggregates. Interconnected grains disrupt progression of contamination forcing harmful ions to travel around the aggregate, which slows corrosion rates. Each mechanism's ability to inhibit corrosion lessens as concrete ages.

2.3.2 Engineered Corrosion Blockers

Engineered technologies can be used in conjunction with concrete's natural corrosion blockers to enhance corrosion inhibition. Technologies currently available include application of coatings or use of methods that change electrochemistry.

Coatings utilize epoxy or metal-based barriers to protect the reinforcement. Epoxy is a polymer that is applied to metals in liquid form and subjected to a curing cycle to form a hard, impenetrable membrane. Due to being impenetrable, contaminants cannot react with the steel to create corrosion products, thus increasing service life. Epoxy coatings require sufficient handling and storage before being implemented into concrete systems which increases labor costs. Poor handling can cause defects or breaks in the membrane that leave steel unprotected in the concrete. Poor storage may lead to the epoxy coating experiencing damage from UV light.

Metal-based barriers act as sacrificial coatings on the reinforcement. Sacrificial coatings utilize the galvanic series and galvanic corrosion to protect metals. The galvanic series is a list of all metals and their measured voltages in solution.

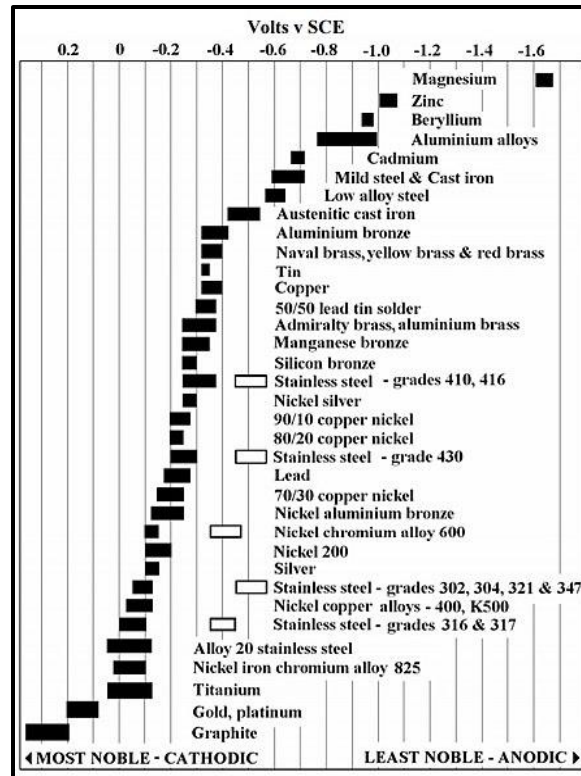


Figure 9 - Galvanic Series of Metals [8]

Galvanic corrosion is the deterioration of a lesser voltage metal when coupled with another metal. A lesser voltage metal will act as an anode and preferentially corrode before the higher voltage metal due to having more favorable oxidation. An anode is a metal surface that loses electrons and promotes oxidation. Cathodes are metals that are protected by anode corrosion. For reinforcement, typically sacrificial coatings comprise of zinc galvanization because zinc has one of the lowest measurable voltages in the galvanic series. Zinc measures between -1.0 and -1.1 V while low alloy reinforcement steel measures between -0.6 and -0.7 V. Galvanizing slows the corrosion of steel reinforcement but is limited because the coating has a finite usability before it is entirely corroded itself. To prolong usability of epoxy and sacrificial coatings, multiple layers can be added [17].

Methods that can change the electrochemistry of corrosion in reinforcement include cathodic protection and impressed currents. Cathodic protection operates under the same mechanism of sacrificial coatings. Instead of a zinc coating on the entirety of reinforcement, zinc pucks are spaced throughout the system. Zinc pucks similarly corrode before steel allowing increased life and are more forgivable in handling and placement [18].



Figure 10 - Zinc Puck Cathodic Protection [18]

Impressed current systems allow the reinforcement to be entirely cathodic resulting in no corrosion. In these systems, reinforcement is attached to a power supply which provides constant current. Constant current restricts the ability for anodic reactions to occur on reinforcement because metals cannot lose electrons. Power supplies are coupled with an external anode that can be easily replaced when corroded. Impressed current systems require total electrical connection of the reinforcement system. If any spot is not in electrical contact with the rest of the system, it could succumb to corrosion. Other disadvantages include the costs of operation and the availability of close power [19].

2.4 Biochar

Biochar is a carbon-based particulate material used for its high adsorptive capabilities. It is the primary byproduct of thermal decomposition of biomaterials or biowastes. Bioproducts include wooden debris from slash piles or lumber mills, remnants of agricultural harvests like corn husk or hemp stock, and animal waste from butcher plants.

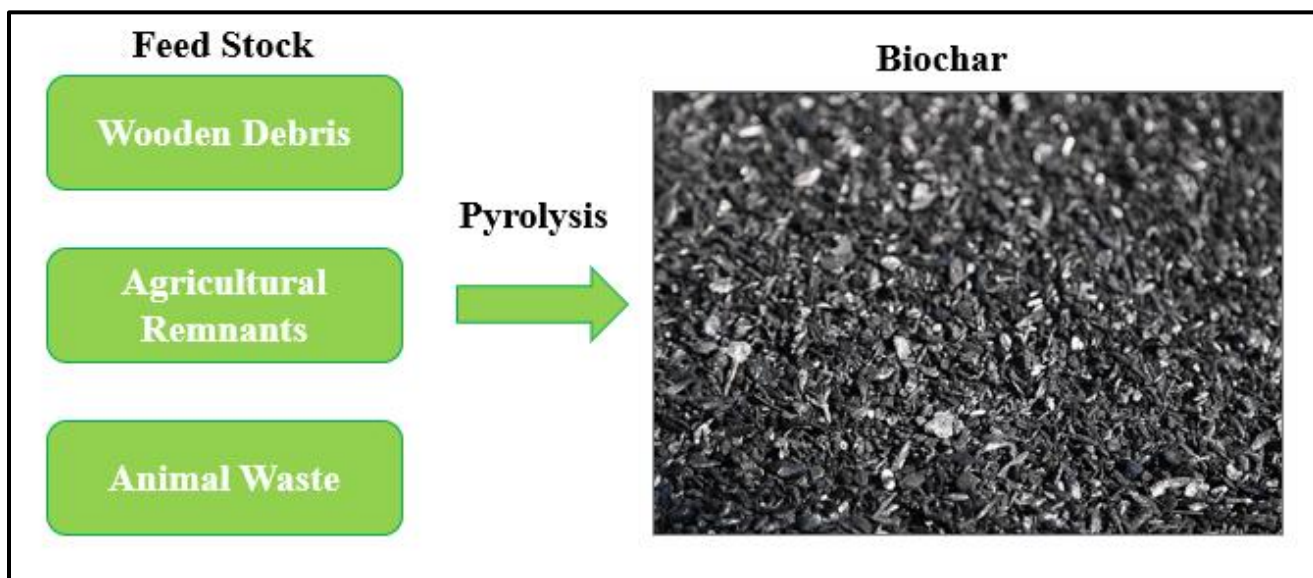


Figure 11 - Biowaste Products for Production of Biochar

One mechanism to achieve thermal decomposition is pyrolysis. Pyrolysis deteriorates biomasses in oxygen deprived environments by breaking chemical compounds and volatilizing residue organic gases present on the bioproduct [20]. Pyrolysis typically occurs at temperatures between 400°C and 800°C (750°F and 1500°F). Inert environments allow the retention of carbon that would otherwise be burned or oxidized as carbon dioxide. Enriched carbon materials have favorable surface chemistry for adsorption due to irregular surface morphology produced from fracturing and volatilizing of biomass under pyrolysis. Favorable surface chemistry characteristics include an increase of surface area and heightened availability for electrostatic attraction [21]. Increased surface area correlates to smaller pore sizes. Smaller pores can trap contaminants

through physisorption. Charged ions present on biochar surface can attract either cationic or anionic contaminants through chemisorption. Both adsorption techniques are seen when placed in concrete.

In addition to its adsorption characteristics, biochar in concrete can influence mechanical properties like strength, density, and emissivity. In terms of strength, one strengthening mechanism relates to the bonding behavior between biochar and cement paste. The irregular surface characteristics of the biochar allow for improved bonding with the hydrated cement creating a more rigid interface. Improved bonding can decrease the susceptibility of crack formation [22]. Strengthening can also be developed through carbonation. Entrapped carbon can react with atmospheric oxygen to initiate the carbonation process. A third strengthening mechanism is due to prolonged hydration. When biochar is integrated within the mix, it adsorbs water. Water retention causes an initial decrease in workability, but, as curing progresses, water can desorb from the biochar to advance cement hydration [22].

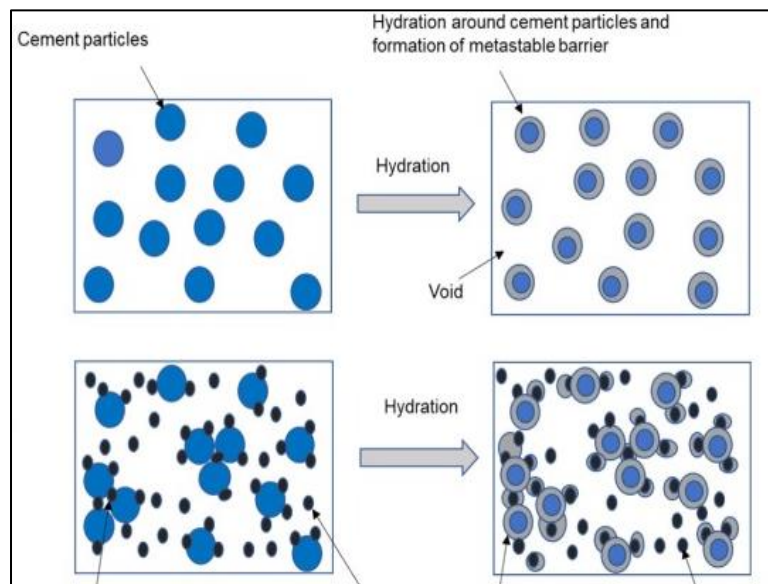


Figure 12 - Prolongation of Cement Hydration Upon Biochar Desorption of Water [22]

In terms of density, when biochar is used as a fine aggregate replacement, bulk unit weight can decrease. Reduced density can be a desired mechanical property because lower dead loads can be achieved within the concrete structure. A dead load is the structures inflicted weight due to gravity. In terms of emissivity, addition of biochar can create a darker surface finish. Emissivity is a measure of effectiveness to emit thermal radiation. Darker materials can emit more induced thermal energy than light colored materials. Highly emissive materials can be desirable in concrete because they can evaporate surface moisture faster. Eliminating surface moisture can also slow progression of corrosion processes [23].

2.5 Bentonite Clay

Bentonite clay is the byproduct of weathered volcanic ash deposits. It is a silica and alumina rich material that can be considered a pozzolan in concrete. American Society for Testing and Materials (ASTM) standard C 618 indicates that pozzolans are, “Siliceous or aluminous materials that by themselves do not exhibit cementitious properties but when mixed with water form compounds that do carry cementitious properties” [24]. Pozzolans can be used as a cement replacement in concrete mixes because they allow cement hydration. Their use can reduce cement production costs and lower emissions from the cement making process. In addition to hydration evolution, bentonite has a large swelling capacity when mixed with water. This characteristic allows formation of a viscous slurry which creates a sealant barrier when dry [25]. Due to its sealing abilities, bentonite is commonly used for natural pond linings or grout casings in wells. Both applications utilize the impervious nature of the clay to prevent water loss in soil. In concrete, it can act as a pore filler and decrease permeability. Pore filling and decreased permeability reduce ingress of harmful contaminants that can initiate corrosion [26].

3.0 Methodology/Materials

To determine the suitability of biochar-bentonite additions in concrete for corrosion resistance, three different testing scenarios were evaluated. These scenarios included, open circuit potential mapping for the determination of corrosion risk, forced migration testing to determine diffusion rate of ingress of harmful salts, and strength testing for the determination of admixtures influence on overall curing reaction. Several mixing ratios of biochar-bentonite (BC:B) were developed for the material testing. In practice, BC:B additions can range from 2-12% by weight of total mixing components. Both biochar and bentonite retain water upon hydration so workability can become a concern in mixing. In addition to reduced workability, excess bentonite integration can cause a decrease in overall strength. Detrimental effects are limited with the use of small admixture ratios[22] [26]. For this research, 4% and 8% by weight ratios were utilized. These ratios account for the total implementation of biochar and bentonite together. Separately, BC:B were mixed in 25:75, 50:50, 75:25 proportions. Ultimately, seven different batches were required, six with BC:B and one control used as a basis for comparison.

Table 1 - Batch Design for Experimental Testing of Corrosion Resistance

	Addition of Admixture by weight	Ratio of Biochar : Bentonite Addition
Batch 1	-	-
Batch 2	4%	75:25
Batch 3	4%	50:50
Batch 4	4%	25:75
Batch 5	8%	75:25
Batch 6	8%	50:50
Batch 7	8%	25:75

3.1 Concrete Mix Design/Mixing

Two different mix designs were utilized for the creation of samples for experimental testing. The first design was for the development of samples for strength and open circuit potential tests. The second design considered additional samples for strength testing along with samples for forced migration testing. Each design was done in accordance with American Concrete Institute standard practice for selecting proportions of concrete constituents (ACI 211.1-91) [24].

Design begins by determining the required volume of samples necessary. Sample sizes in each batch of mix one included three, 30cm x 30cm x 10cm (12in x 12in x 4in) slabs and one 10 cm (4in) diameter by 20cm (8in) cylinder. Sample sizes in each batch of mix two included, five cylinders and one 15cm x 15cm x 52.5cm (6in x 6in x 21in) beam. Table 2 below indicates the necessary volume needed for one batch in each mix. Seven batches for each mix were created.

Table 2 - Concrete Volume Required for Sample Creation

	Volume Required m ³ (ft ³)
Mix 1	0.029 (1.05)
Mix 2	0.034 (1.20)

Once net volume was determined, assumptions for design could be made. Assumptions include choice of desired slump, maximum size of aggregate used, estimation of mixing water and air content, determination of fineness moduli, estimation of coarse unit weight, and selection of water to cement ratio.

Slump relates to the workability of concrete. It is an index of the fluidity of the components after mixing. Slump is measured by determining the amount of deformation that occurs when a conical mold is released from the wet concrete and the wet concrete can fall in on itself. It is desirable to have enough fluidity so concrete can be sufficiently transported through

reinforcement systems. Type of construction dictates desired slump. For reinforced beams, walls, and columns, typical values of slump range from 75mm to 100mm (3in to 4in) [27]. The maximum sized aggregate used was 19mm (0.75in). This was based on material available for use. These two elements along with a designation of assumed air exposure dictate the estimation of bulk mixing water per table 6.3.3 in ACI 211. Severe air exposure is typical for concrete that is exposed to harmful chemicals like deicing agents or other aggressors. Based on these assumptions, it is estimated that 184 kg/m^3 (305 lb/ft^3) of water is required for mixing. The fineness modulus is the ratio between volume of coarse aggregate per volume of concrete and helps in the determination of how much fine aggregates are needed in the mix. A value of 2.7 is assumed. This number and the slump dictate the ratio of fine and coarse aggregates per table 6.3.6 in ACI 211. The result is 0.63, which means that for every 100 units of weight for coarse aggregate there are 63 weight units of fine aggregates. Finally, the water to cement ratio is determined based on desirable properties of the finished concrete. In this case a water to cement ratio of 0.45 was assumed. Annex 6.1 depicts necessary design tables for designing per ACI 211. Other assumed numbers for calculation include the specific gravities of cement, coarse aggregate and fine aggregate, and unit weights of water and of the coarse aggregate. Cement has a specific gravity of 3.15 while coarse and fine aggregates are 2.75 and 2.68 respectively. Water has a unit weight of 1000 kg/m^3 (62.4 lb/ft^3) and coarse aggregates have a unit weight of 1600 kg/m^3 (100 lb/ft^3).

When all the design assumptions have been made, computation can be done with all the developed numbers. Weight of water is derived first. This calculation is the product of the total volume required times the estimation of mixing water.

$$\mathbf{Water\ Weight = (Volume\ Required) (Bulk\ Mixing\ Water)}$$

Equation 4 - Water Weight Calculation

Next is the derivation of the cement weight. To calculate this value, the water weight is divided by the desired water to cement ratio.

$$\mathbf{Cement\ Weight = \frac{Water\ Weight}{W:C}}$$

Equation 5 - Cement Weight Calculation

Next is the derivation of fine aggregate weight. The ratio of fine to coarse aggregate is multiplied with the coarse aggregate unit weight and the volume required.

$$\mathbf{Fine\ Aggregate\ Weight = \left(\frac{fine}{coarse}\right) (Coarse\ Unit\ weight) (Volume\ Required)}$$

Equation 6 - Fine Aggregate Weight Calculation

After these weights have been established, their respective volumes can be determined.

Component volume is equal to the weight divided by the product of specific gravity (SPG) and unit weight of water (ρ).

$$\mathbf{Component\ Volume = \frac{Component\ Weight}{(SPG) (\rho)}}$$

Equation 7 - Component Volume Calculation

The volume of air is assumed to be 6% of the total volume required for the mix and relates to the air exposure criteria. Air volume is then summed with each other component and subtracted from the total volume of concrete required. This determines the necessary volume of coarse aggregates required.

$$\mathbf{Coarse\ Aggregate\ Volume = Volume\ Required - \sum Component\ Volume}$$

Equation 8 - Coarse Aggregate Volume Calculation

Coarse aggregate weight is the final calculation for basic mixes. It is the product of the coarse aggregate volume, coarse aggregate specific gravity, and unit weight of water.

$$\mathbf{Coarse\ Aggregate\ Weight = (Coarse\ Aggregate\ Volume) (SPG) (\rho)}$$

Equation 9 - Coarse Aggregate Weight Calculation

Modifications can be made to each of the aggregate weights and to the water weight based on aggregates retention of water. Water retention occurs when sands and gravels are stored outside. Fluctuations in weather can influence moisture content of the aggregates. To compute a modified aggregate weight and water weight it is necessary to obtain absorption capacity and moisture content percentages. Absorption capacity is the maximum amount of water aggregates can retain. It is the percent difference between saturated surface-dry weight and oven dried weight. Saturated surface dry weight is the weight of aggregates that are dry to the touch but contain water in their microstructural pores. Oven drying drives off excess moisture reducing the weight of the aggregate.

$$\mathbf{Abs = \frac{Wt_{SSD} - Wt_{OD}}{Wt_{OD}}}$$

Equation 10 - Absorption Capacity Calculation

Moisture content is the ratio of total wet weight to dry weight. Moisture contents account for moisture that can reside on the surface of the aggregate. Absorption capacity and moisture content can either be derived experimentally or can be listed on material specifications from an aggregate supplier. Table 3 indicates the values given by Pioneer Rock and Sand Supply.

Table 3 - Absorption Capacity and Moisture Content for Aggregates Used in Mix Design

	Abs	MC
Gravel	0.60%	1
Sand	1.20%	1.019

Modified aggregate (W_{CA} and W_{FA}) weight can be calculated by multiplying the original weight by a function of the absorption capacity and the moisture content.

$$\mathbf{Modified\ Aggregate\ Weight} = (\mathbf{Aggregate\ Weight}) \frac{((\mathbf{1})(\mathbf{MC}))}{(\mathbf{1} + \mathbf{Abs})}$$

Equation 11 - Modified Aggregate Weight Calculation

If there is excess water retention in the aggregate and the water weight is left uncorrected water to cement ratios can be altered influencing cement hydration and overall strength. The modified water weight (W_{wa}) is equal to the sum of the original weight components minus the cement weight and each of the modified aggregate weights.

Modified Water Weight

$$= \sum \mathbf{Component\ Weight} - \mathbf{Cement\ Weight}$$

$$- \sum \mathbf{Modified\ Aggregate\ Weight}$$

Equation 12 - Modified Water Weight Calculation

With the additions of biochar and bentonite further modifications can be computed. Biochar is assumed to act as a fine aggregate replacement [22]. Bentonite is assumed to act as a cement replacement [26]. The resulting mix designs can be seen in tables 4 and 5 below.

Table 4 – Mix Design for Mix 1 Samples

	Addition by weight	Ratio of BC : B	BC Weight kg (lb)	B Weight kg (lb)	Water Weight kg (lb)	Fine Aggregate Weight kg (lb)	Coarse Aggregate Weight kg (lb)	Cement Weight kg (lb)
Batch 1	-	-	0	0	14.6 (32.2)	21.0 (46.4)	20.8 (45.8)	12.0 (26.5)
Batch 2	4%	75:25	2.1 (4.6)	0.7 (1.6)	14.6 (32.2)	19.0 (41.9)	20.8 (45.8)	11.3 (25.0)
Batch 3	4%	50:50	1.4 (3.0)	1.4 (3.0)	14.6 (32.2)	19.7 (43.4)	45.8 (20.8)	10.6 (23.4)
Batch 4	4%	25:75	0.7 (1.6)	2.1 (4.6)	14.6 (32.2)	20.4 (44.9)	45.8 (20.8)	10.0 (22.0)
Batch 5	8%	75:25	4.1 (9.0)	1.4 (3.0)	14.6 (32.2)	17.0 (37.4)	45.8 (20.8)	10.6 (23.4)
Batch 6	8%	50:50	2.7 (6.0)	2.7 (6.0)	14.6 (32.2)	18.3 (40.4)	45.8 (20.8)	9.3 (20.4)
Batch 7	8%	25:75	1.4 (3.0)	4.7 (10.4)	14.6 (32.2)	19.7 (43.4)	20.8 (45.8)	7.3 (16.0)

Table 5 - Mix Design for Mix 2 Samples

	Addition by weight	Ratio of BC : B	BC Weight kg (lb)	B Weight kg (lb)	Water Weight kg (lb)	Fine Aggregate Weight kg (lb)	Coarse Aggregate Weight kg (lb)	Cement Weight kg (lb)
Batch 1	-	-	0	0	16.4 (36.7)	24.0 (52.8)	23.6 (52.1)	13.7 (30.1)
Batch 2	4%	75:25	2.4 (5.2)	0.8 (1.7)	16.4 (36.7)	21.6 (47.6)	23.6 (52.1)	12.9 (28.4)
Batch 3	4%	50:50	1.5 (3.4)	1.5 (3.4)	16.4 (36.7)	22.4 (49.3)	23.6 (52.1)	12.1 (26.7)
Batch 4	4%	25:75	0.8 (1.7)	2.4 (5.2)	16.4 (36.7)	23.2 (51.1)	23.6 (52.1)	11.3 (25.0)
Batch 5	8%	75:25	4.7 (10.3)	1.5 (3.4)	16.4 (36.7)	19.2 (42.4)	23.6 (52.1)	12.1 (26.7)
Batch 6	8%	50:50	3.1 (6.9)	3.1 (6.9)	16.4 (36.7)	20.8 (45.9)	23.6 (52.1)	10.6 (23.3)
Batch 7	8%	25:75	1.5 (3.4)	4.7 (10.3)	16.4 (36.7)	22.4 (49.3)	23.6 (52.1)	9.0 (19.8)

Mixing of the batched components was done in accordance with ASTM standard C94 [28]. A 1.1 m³ (1.5 yd³) capacity stationary drum mixer was used for the mixing. This drum mixer rotates materials at 1725 RPM. Water and cement are the first constituents added to the drum. Application of water allows for wetting of the drum walls, so powdered cement or biochar and bentonite do not stick and become unmixed. After water and cement, the biochar, bentonite, and fine aggregates were added. Coarse aggregates were the last component in the mixer. Mixing time is measured once all components are placed in mixer. Mix time is at least 1 min per 0.76 m³ (1yd³). This time allows for sufficient wetting of all components. After mixing concluded, the wet concrete was added to molds and placed in a cure room. Cure rooms have a controlled humidity and temperature to mimic optimal environmental characteristics for placed concrete. A room temperature of 20°C (72°F) and humidity of 99% are ideal for optimal curing of concrete. High humidity is desired to maintain water so cement hydration can be prolonged to full curing [1].

3.2 Open Circuit Potential Testing

Several methods of nondestructive examination are used to evaluate corrosion of reinforcement systems where visual indicators may be in concentrated quantities or not present at all. One tool utilized in routine inspections of concrete structures is the method of Open-Circuit Potential mapping (OCP).

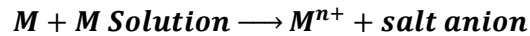
OCP is a measure of the induced voltage supplied by a reference electrode on to reinforcement systems. Measurements are made in accordance with ASTM standard C876 [29]. This process works through half-cell electrochemical reactions within the reference electrode and an electrical contact with in-place rebar. To test existing structures, local destruction is required to maintain electrical contact with the reinforcement. Half-cell reactions are derived from the central metal rod and metal-based solution which are found in the electrode. Metal rods, designated M, are often materials that have good conductive properties and can easily transfer charged particles. Metal decomposes into charged cations with n-charge and n-electrons. The metal-based solution interacts with n-electrons to create more metal cations as well as salt anions. Coupled together, these half-cell reactions yield an overall reaction which can be used in conjunction with the Nernst equation to determine the standard potential voltage difference $E^0_{M/M-soln}$. Reference electrodes are typically comprised of silver/silver chloride (SSC) or copper/copper sulfate (CCS). A CCS electrode was used for this application as that is widely used in industry. The Nernst equation utilizes the ideal gas constant R, number of electrons involved in the half cell reactions N, and Faradays constant F. The standard potential difference is related to the measured voltage between the electrode and the rebar.



Equation 13 - Anodic Half-Cell Reaction in Reference Electrodes



Equation 14 - Cathodic Half-Cell Reaction in Reference Electrodes



Equation 15 - Net Half-Cell Reactions for Reference Electrodes

$$E = E_{M/Msoln}^0 - \frac{RT}{nF} \ln \left[\frac{\text{Products}}{\text{Reactants}} \right]$$

Equation 16 - Nernst Equation for Net Half-Cell Reaction

The electrode also has a ceramic plug which provides a pathway for diffusing electrons in testing. Around the plug is a conductivity sponge which serves as an electrical bridge between the concrete surface and the electrode [30].

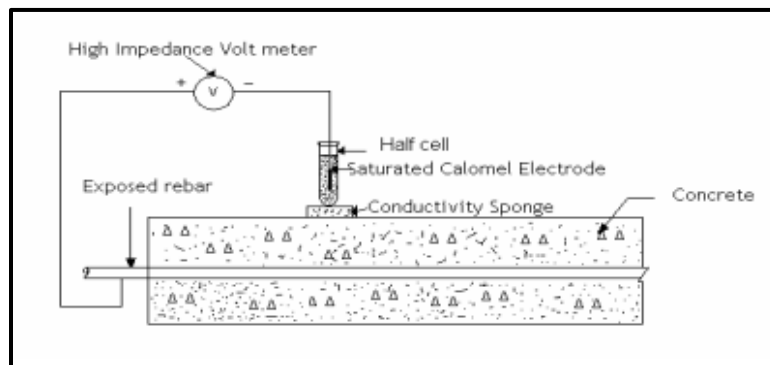


Figure 13 - Schematic of OCP Test [30]

As metal in the reference electrode undergoes oxidation, electrons can travel to the reinforcement. Upon acquisition of traveling electrons, iron in the steel dissociates into charged iron cations. This dissociation correlates to a voltage change that can be read from a voltmeter.

Table 6 - Corrosion Risk Severity Criterion

Corrosion Severity	Potential Difference vs CCS
severe corrosion	<-500 mV
high (90% risk)	<-350 mV
intermediate risk	-200 mV < x < -350 mV
low risk	>-200 mV

OCP mapping is useful because it creates a hot map of where corrosion is likely to occur within a structure. If corrosion severity is concentrated in small areas, rehabilitation efforts can be put in place. If an entire structure has a high risk of corrosion, large scale rehabilitations or replacement considerations should be made.

OCP testing for the biochar-bentonite mixes was done on slabs with reinforcement protruding from the concrete. Protruding reinforcement allowed for easier OCP measurement. One slab from each batch was placed in solutions of 1M NaCl, Na₂SO₄, and Ca(OH)₂. The concentration of each solution was set at 1M to ensure noticeable changes could be observed in a timely manner. M indicates molar concentration, which is the ratio of molar weight (mol) of salt per volume of water (L). Molar weight is the weight of 1 mol of a substance. These weights can be obtained directly from a periodic table.

$$\text{Molar Concentration} = \frac{\frac{\text{Weight of Salt}}{\text{Molar Weight}}}{\text{Volume of Solution}}$$

Equation 17 - Molar Concentration Calculation

NaCl mimicked exposure of chlorides, Na₂SO₄ mimicked exposure to sulfates, and Ca(OH)₂ mimicked natural conditions of concrete. Slabs were alternated between the wet solution and a dry environment every 3-4 days to mimic changing environmental conditions concrete structures experience in their service lives. Upon each alternation, OCP was measured. Alternations

followed a cycle of submersion for 4 days, drying for 4 days, submersion for 3 days and drying for 3 days. Each cycle was 2 weeks in length and there were 6 sequential cycles in total [31].



Figure 14 - Samples in Solution for Wet OCP Measurements

3.3 Forced Migration Testing

Forced migration testing analyzes the diffusion of chloride ions through concrete. Diffusion rates can be helpful in the determination of how fast corrosion processes occur in reinforcement. In this test, a concrete disk acts as a boundary layer between a saturated saltwater tank and an unsaturated water tank. Graphite sheeting is placed in each tank to act as electrodes. Graphite is used because it is the material least prone to corrosion in saltwater on the electromotive force series, see figure 9 above. This ensures the electrodes can stay intact during testing. A constant voltage battery pack is applied to each electrode and forces the salt anions available in the saturated tank through the concrete into the unsaturated tank. Salt transport is driven by an electric field that is developed between the two electrodes. Upon application of electric charge, the saturated tank is the catholyte and the saturated tank is the anolyte. The positive electrode is placed in the anolyte tank and attracts the negatively charged salt anions. A detailed schematic

and 3D views of the system can be seen in figures 15-17. Natural diffusion can occur in the system due to concrete having porous microstructure, but this process could take weeks to months for any noticeable concentration changes to occur. Forced migration allows for faster recognition of changes of concentrations in the system [32].

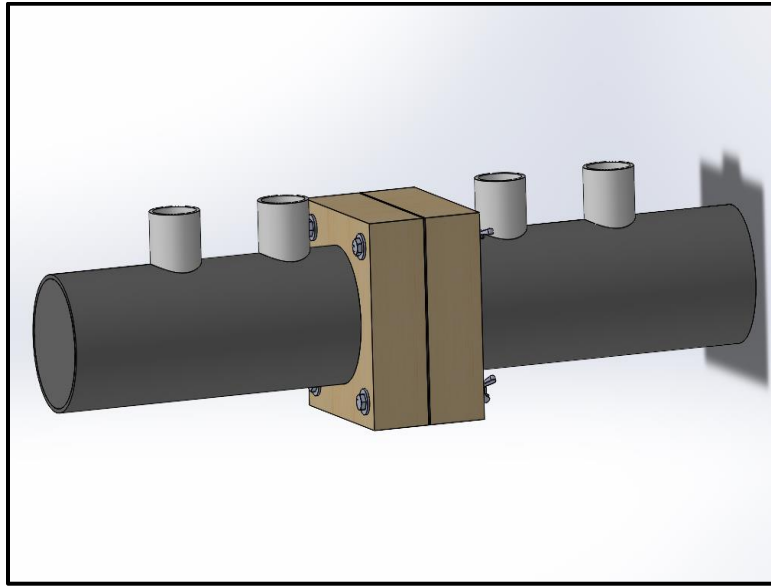


Figure 15 - 3D Solid Model of Diffusion Cell

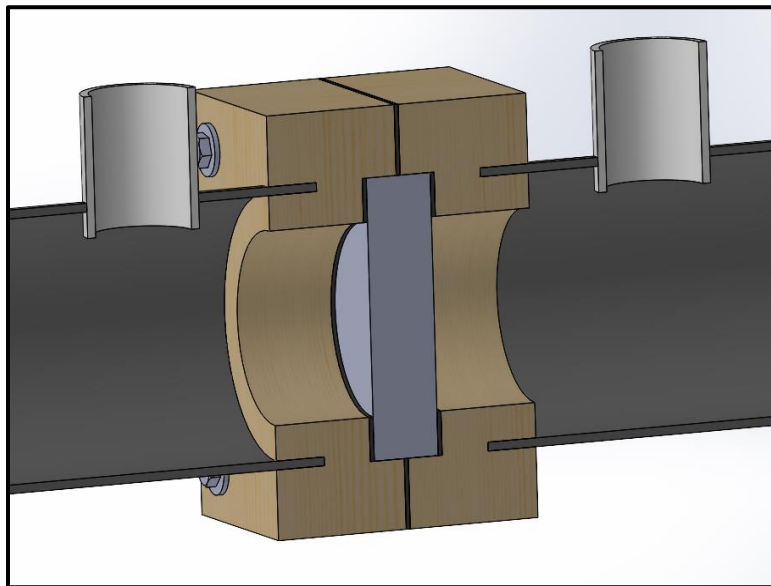


Figure 16 - Internal Section View of 3D Solid Model

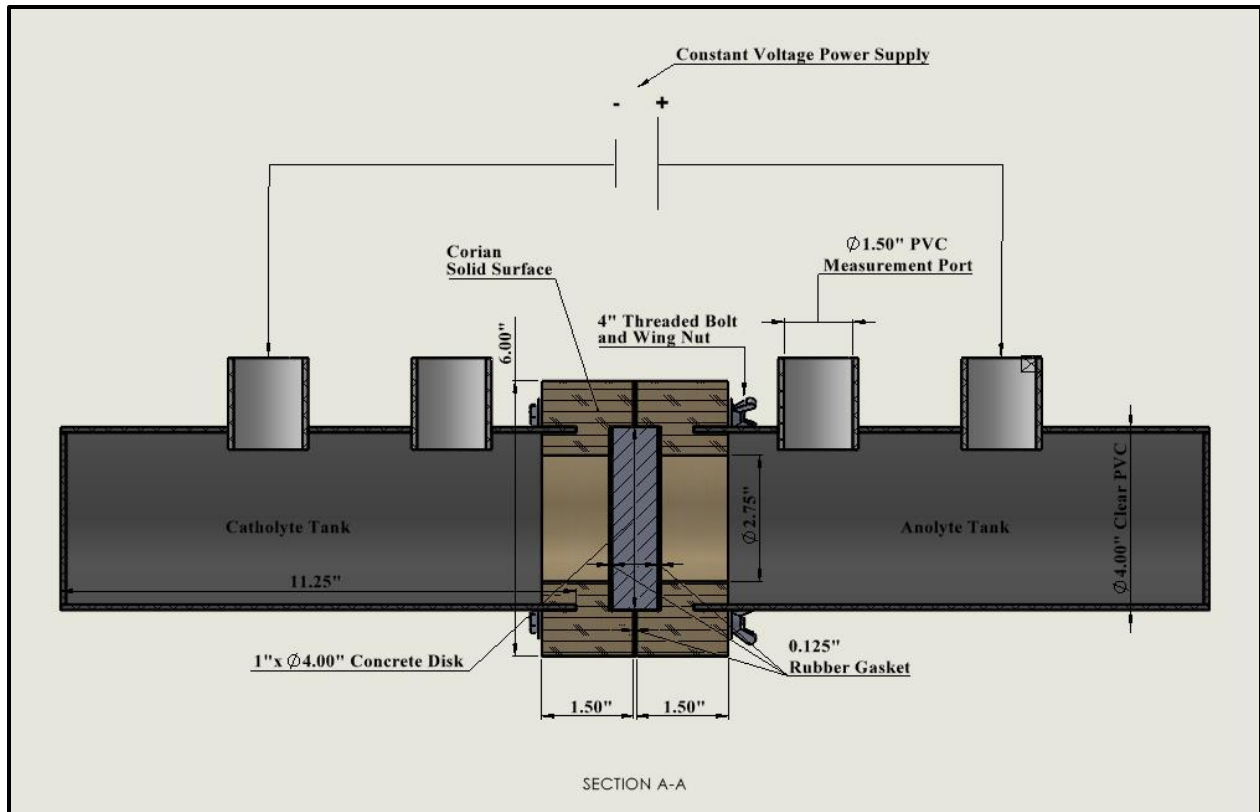


Figure 17 - Diffusion Cell Section and Details

The concentration change of the anolyte tank can be tracked by measuring the conductivity of the solution with respect to time. Saline solutions are good conductors for electrical current because salt ions can carry electric charge. With more ions in solution, conductivity can increase. The relationship between concentration and conductivity is a direct proportionality [33]. An experimental conductivity profile of NaCl saltwater was developed to evaluate concentration change with respect to time in the anolyte tank. For this profile, concentrations varied between 0 and 1.2 M while conductivities varied between 0.016 and 93.8 mS, where mS is milli Siemens. The range of 0 to 1.2 is utilized because the catholyte tank is initially 1 M. This concentration mimics seawater conditions [32]. Different concentrated solutions were created with different weight additions of NaCl in 500 mL of deionized water. Deionized water is water that has been filtered to limit the amount of trace ions. Trace ions from unfiltered water could influence

inaccurate conductivity measurements. Deionized water was used both for the profile and for testing. The profile developed is seen in Figure 18 below. From this profile, a conversion equation could be applied to conductivity measured in the anolyte tank.

Table 7 - Molar Concentration and Conductivity for Profile Development

Molar Concentration M	Conductivity mS
1.2	93.8
1	80.3
0.8	65.7
0.6	52.2
0.4	35.6
0	0.016

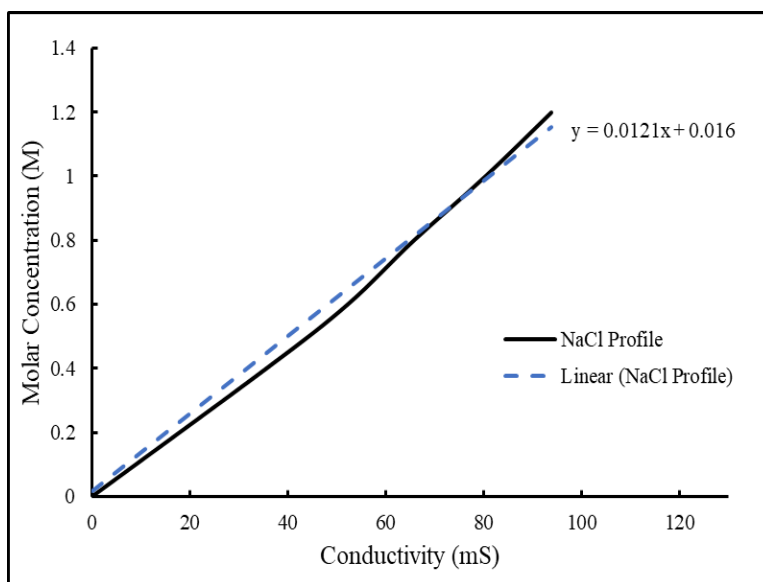


Figure 18 - Conductivity vs Concentration Profile for NaCl

Conductivity measurements were taken with a YSI model 30 Handheld Conductivity probe. Calibration of the probe was done with conductivity standard solution each week. Calibration for systems that mimic seawater utilize a standard that has 1.413 mS [34].

For the sample testing, conductivity measurements were taken every 8 to 10 hours. This ensured sufficient curvature could be reflected for the change in concentration versus time curve [32]. Typical concentration versus time curves for concrete diffusion portray three distinct regions, an equilibrium plateau, slope of concentration gradient, and a binding plateau. The binding plateau at the beginning of the curve occurs because chloride can initially bind with the cement matrix of the concrete. When salt ions are free and unable to further bind the slope of concentration gradient begins. This region of the curve dictates the rate of changing concentration. After enough time has past, the diffusion system equilibrates which can usually occur around half of the magnitude of the initial catholyte concentration. A typical concrete curve can be seen in Figure 19 below.

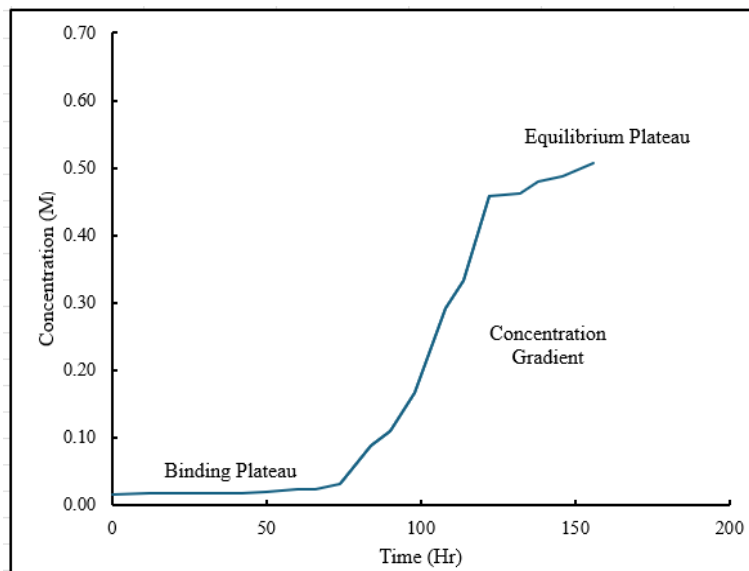


Figure 19 - Typical Diffusion Curve for Concrete

The slope associated with the concentration gradient region of the curve is used to determine the coefficient of diffusion for the chloride through concrete. Slope over diffusion area gives flux (J) of the system. Diffusion is a function of flux, sample thickness (L), applied voltage (V), temperature (T), initial catholyte concentration (C_0), and charge of anion (z). A typical value for

normal 0.45 w:c concrete is $1.55 \times 10^{-4} \text{ cm}^2/\text{hr}$ ($2.40 \times 10^{-5} \text{ in}^2/\text{hr}$). However, it should be noted that this value can be variable based on different curing conditions, mixing practice, and material handling [32].

$$D = \frac{J R T L}{V F C_0 Z}$$

Equation 18 - Diffusion Coefficient Calculation

Table 8 - Constants for Calculation of Diffusion Coefficient

Constants	Value	Units
Electric Charge (z)	1	n/a
Faradays Constant (F)	96500	coulomb/mol e-
Voltage (V)	14.6	Volts
Thickness (L)	2.54 (1)	cm (in)
Gas Constant (R)	8.3145	J/mol K
Temperature (T)	295	K
Area	31.66 (4.91)	cm ² (in ²)

3.3.1 Diffusion Cell Construction

To construct the diffusion cell, clear PVC piping was used for the tanks. Clear PVC allowed for each tank to be viewed during testing. Smaller PVC piping was used for the electrode and measurement ports on each tank. Gaskets were used to seal the system when put together. An iterative design process was used for the cell housing of the concrete disk. The first design utilized a circular built up section of maple hardwood coated with sealant. Maple hardwood was used because it has a tight grain structure preventing water leaking. Sealant around the maple was theorized to further prevent water leaks. Upon joining with the PVC piping, the bond did not hold. A latex based caulking was used and did not adhere to the silicon-based sealant. Another issue in this design was there was not enough clamping pressure from the fastening bolts on the section. In the second design, a square built up section of maple hardwood was used, and sealant

was applied everywhere but the joining surface with the PVC. The square shape allowed for more clamping pressure from the tightening of the bolts. A silicon-based caulking was used instead of the latex caulking, which gave a better bond. This system held water, initially. After 12 hours, the water that had held in the system infiltrated the sealed wood. This issue called for a third design. For this, a square built up section of corian solid surface was used. Corian is a material that is used for countertops and is waterproof. Again, the exterior was sealed for further protection against leaking and the housing was joined to the PVC with silicon-based caulking. External leaks of the system were mitigated however, in a few cells, internal leaking was occurring. To mitigate this issue, different types of gaskets were used, and hot glue was applied to the concrete in the housing. The different types of gaskets were rubber and viton sheeting. Viton sheeting was less rigid and could conform with any minor irregularities from cutting of the concrete disks. Disks were cut with a diamond bladed tile saw. Each disk was cut to 2.5 cm (1in) thick.

3.4 Strength Testing

To evaluate each admixtures influence on strength, compressive and flexural stress were analyzed. Compression testing was done on the 10 cm (4in) cylinders while flexural testing was done on the 15cm x 15cm (6in x 6in) beams. Each test was done on 28-day cured samples. After 28 days samples have reached at least 95% of full strength. Ultimate compressive stress was analyzed in accordance with ASTM C39 [35]. Testing was performed in a Humbolt 69000 kPa (10000psi) load frame.



Figure 20 - Compressive Strength Test Frame

Samples were coupled with a rubberized pad to conform to any surface irregularities present from casting. The pads also ensured that testing was done perpendicular to the cross-sectional area. Each sample was tested with a loading rate of 275 kPa/s (40 psi/s). The slow loading rate limits material shock from force application. Material shock can negatively influence strength characteristics. Testing stops once a peak load is achieved and the load decreases to 80% of the maximum value. Compressive strength is the ratio of peak loading to the cross-sectional area. This value is critical in the determination of stiffness of the concrete system. Cylinder failures upon loading appear in a conical shape, which is due to shearing rupture.

$$f_c' = \frac{\text{Peak Load}}{\text{Cross - Sectional Area}}$$

Equation 19 - Compressive Stress Calculation

Maximum bending stress was tested in accordance with ASTM C78 [36]. Testing was done in a Enerpac P142 69000 Kpa (10000psi) frame. This frame utilizes manual loading from a hydraulic

jack. A 4-pt bending apparatus is used to maximize bending of the loaded region of the specimen.



Figure 21 - 4-Pt Bending Strength Tests

Specimens are created such that there is a 3:1 span to depth ratio. The span length is 45 cm (18in) which is three times the depth of each beam. Testing is carried out until the specimen breaks. Failure will occur on the bottom of the beam where maximum tension is felt. From peak loading, a maximum moment can be determined. Max moment is equal to the peak load times the span length over six. Bending stress is the maximum moment times the centroid of the shape over the area moment of inertia. The centroid is the point where no compression or tension force is felt within the shape of the beam. For a square shape the centroid acts at the center. The area moment of inertia is the area that resists bending.

$$M_{max} = \frac{P L}{6}$$

Equation 20 - Maximum Moment for 4-Pt Bending

$$\sigma_b = \frac{M_{max} c}{I}$$

Equation 21 - Bending Stress Calculation

4.0 Results/Discussion

4.1 Mixing

Upon the mixing of batch 1 in mix 1, it was observed that the mix design called for too much water. Too much water was evident by a non-viscous slurry of hydrated cement. When mixing, concrete should have a viscous consistency like peanut butter, which has high resistance to flow but can be easily worked. This batch was ultimately scraped and redone. To limit potential for too much water in subsequent batches, water was added incrementally until a desired slump was achieved. Each slump was maintained at approximately 15 cm (6in). Due to the water retention of the biochar and the bentonite, water content utilized for consistent fluidity was high and lead to high water to cement ratios. Tables 9 and 10 below detail those values.

Table 9 - Mix 1 Actual Water Weight, Slump, and W:C

	Addition by weight	Ratio of BC : B	Design Water Weight kg (lb)	Actual Water Weight kg (lb)	Slump cm (in)	W:C
Batch 1	-	-	14.6 (32.2)	5.9 (13.0)	17.2 (6.75)	0.49
Batch 2	4%	75:25	14.6 (32.2)	9.5 (21.0)	15.9 (6.25)	0.84
Batch 3	4%	50:50	14.6 (32.2)	11.3 (25.0)	15.9 (6.25)	1.06
Batch 4	4%	25:75	14.6 (32.2)	12.0 (16.4)	15.9 (6.25)	0.74
Batch 5	8%	75:25	14.6 (32.2)	15.2 (33.5)	16.5 (6.5)	1.43
Batch 6	8%	50:50	14.6 (32.2)	14.5 (32.0)	16.5 (6.5)	1.56
Batch 7	8%	25:75	14.6 (32.2)	15.9 (35)	15.9 (6.25)	2.18

Table 10 - Mix 2 Actual Water Weight, Slump, and W:C

	Addition by weight	Ratio of BC : B	Design Water Weight kg (lb)	Actual Water Weight kg (lb)	Slump cm (in)	W:C
Batch 1	-	-	16.4 (36.7)	6.8 (15.0)	14.0 (5.5)	0.49
Batch 2	4%	75:25	16.4 (36.7)	11.3 (25.0)	17.2 (6.75)	0.88
Batch 3	4%	50:50	16.4 (36.7)	10.4 (23.0)	15.2 (6.0)	0.86
Batch 4	4%	25:75	16.4 (36.7)	8.2 (18.0)	14.6 (5.75)	0.72
Batch 5	8%	75:25	16.4 (36.7)	10.9 (24.0)	15.2 (6.0)	0.89
Batch 6	8%	50:50	16.4 (36.7)	13.2 (29.0)	14.0 (5.5)	1.24
Batch 7	8%	25:75	16.4 (36.7)	17.7 (39.0)	14.0 (5.5)	1.96

4.2 Open Circuit Potential Test

Surface appearance of each slab was inspected prior to OCP testing, this acted as a baseline comparison when evaluation was completed. An initial smooth surface finish was observed for each slab. Pore pockets were observed on each sample but quantity and size varied. Small pores occurred on the control and 4% by weight samples while larger pores occurred on the 8% by weight samples. This phenomenon was due to higher w:c ratios in the mixing process. As testing progressed, a record of physical appearance was maintained. Typical observations included growth of efflorescence staining, formation of rough surface due to salt scaling, propagation of cracking, and small spalling of the corners. Efflorescence staining likely occurred due to alternation of wet and dry cycles. Any excess moisture that was retained during the wet cycle evaporated in the dry cycle. Salt scaling is the attack of the surface finish of the concrete. De-cementation can occur leaving a rough outer surface on the concrete. Scaling was more evident on the samples submerged in Na_2SO_4 . Sodium sulphate exhibits a larger molecular size than NaCl and $\text{Ca}(\text{OH})_2$ so more aggressive attack can occur. An example of scaling can be seen in Figure 22 below.



Figure 22 - Example of Typical Salt Scaling on Na_2SO_4 Samples

Cracks were able to propagate because reinforcement was likely enduring rust formation. Cracks were observed when potential voltage readings indicated severe corrosion risk. Spalling occurred due to the coalescence of cracking on the slab. For the potential voltage readings, typical peaks and valleys can be recognized in Figures 24-26. These fluctuations are due to the alternation of wet and dry readings. Valleys correlate with dry cycles and peaks correlate with wet cycles.

For samples submerged in NaCl, the control slab exhibited the slowest rate of change of corrosion risk. This could be due to the small number of observed pores at initial inspection. The next slowest rate of changing corrosion risk was the 4 – 75:25 mixture. Intermediate risk occurred after approximately 60 days of testing. Each of the other mix ratios were in the severe risk category after 28 to 45 days of testing. Corrosion risk vs time curves of samples submerged in NaCl can be seen in Figure 24. Data for the development of the curves can be found in Appendix 6.3.1. After OCP testing, each slab was broken open to expose the condition of the reinforcement. Heavy presence of corrosion products could be seen on the samples with the most bentonite, this correlated with the more negative potential values indicating severe corrosion risk. Limited corrosion products were observed on the samples with higher biochar content, this correlated with potential values in the low or intermediate risk range. The control showed no initiation of corrosion products.

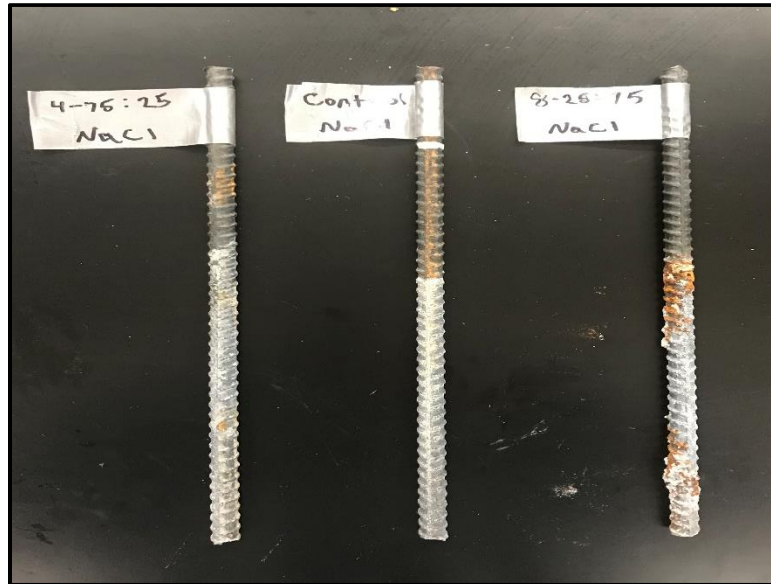


Figure 23 - Reinforcement from Slabs in OCP Testing

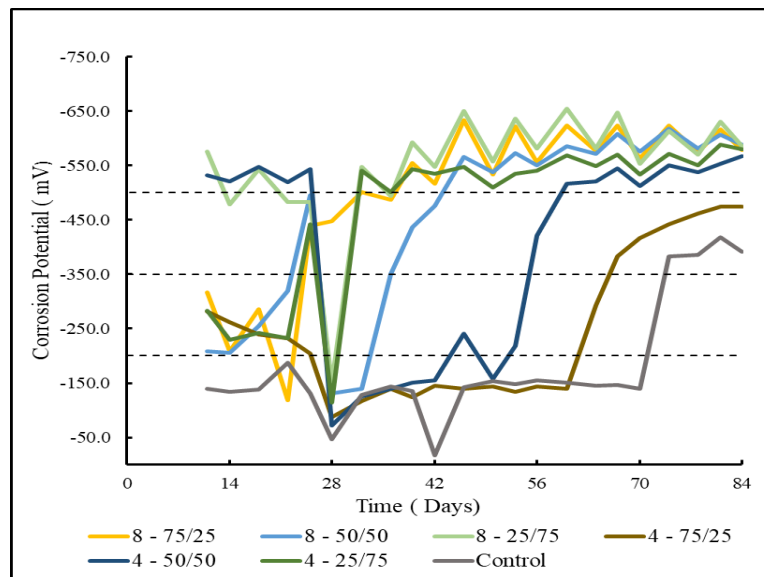


Figure 24 - Potential vs Time for Samples in NaCl

For samples submerged in $\text{Ca}(\text{OH})_2$, again the control exhibited the slowest change of corrosion risk. Each of the 75:25 ratios for the 4% and 8% weight additions were the next slowest. Both samples only reached a high corrosion risk after 50 days of testing. All other samples portrayed

severe corrosion risk after 28 days. Corrosion risk vs time curves of samples submerged in $\text{Ca}(\text{OH})_2$ can be seen in Figure 25. Data for the development of the curves can be found in Appendix 6.3.2.

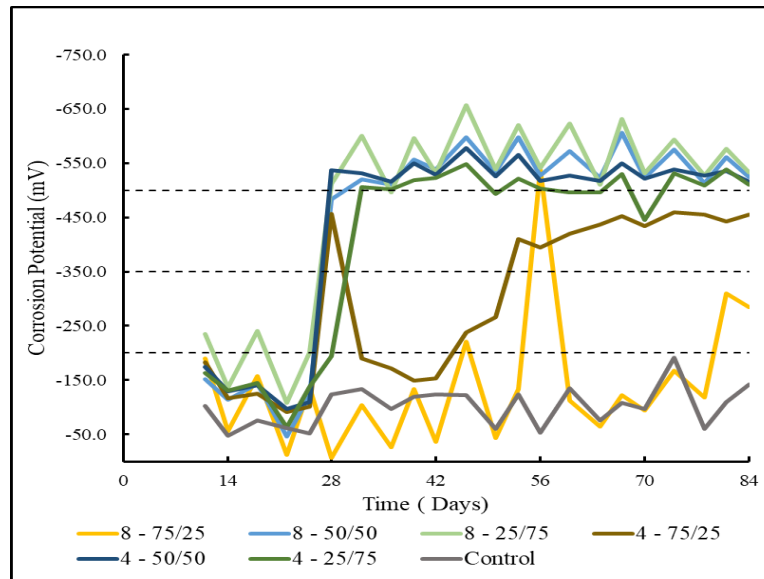


Figure 25 - Potential vs Time for Samples in $\text{Ca}(\text{OH})_2$

For samples submerged in Na_2SO_4 , again the control was slow in corrosion risk advancement. All the 4% weight ratio mixes were also slow in progression and only stayed in the low-risk range. Each of the 8% weight ratio mixes experienced faster risk development between 28 and 45 days. Corrosion risk vs time curves of samples submerged in Na_2SO_4 can be seen in Figure 26. Data for the development of the curves can be found in Appendix 6.3.3. Reinforcement within the Na_2SO_4 experienced less risk of corrosion advancement overall. This was evident by more samples in the low-risk range at the conclusion of testing. However, the concrete surface showed signs of more aggressive deterioration from salt scaling. Reinforcement condition was also evaluated by breaking the concrete slabs. Similarly to the reinforcement in NaCl samples, samples with elevated bentonite addition portrayed heavy corrosion products while samples with

elevated biochar addition had limited products. Control in Na_2SO_4 also had no initiation of corrosion products.

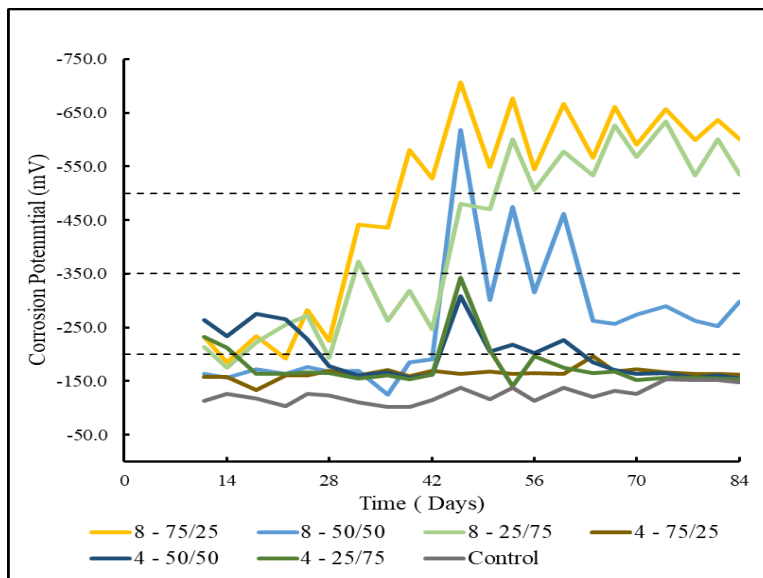


Figure 26 - Potential vs Time for Sample in Na_2SO_4

4.3 Forced Migration Test

With the built-up corian diffusion cell, testing was able to progress. Each sample was tested at least twice to establish a mean flux and diffusion coefficient. Duplicate measurements were run to limit the influence of variability on testing. Some samples experienced short circuiting while testing. Short circuiting was indicated by fast changes in conductivities and concentration at the start of testing. Steep concentration gradients on the concentration vs time curves can be seen from short circuiting. Short circuiting could occur due to two potential mechanisms. The first was due to narrow gaps between the minor irregularities of the surface of the concrete and the gasket material. Minor irregularities arose from imperfections in cutting of the disks. The second mechanism for short circuiting was due to the presence of large pore pockets near the disk edges. Narrow gaps between concrete surface and gasket material were limited with the use of the more pliable viton sheeting. Large edge pore pockets were filled with hot glue. In most samples, no

binding plateau was evident on the concentration vs time curves. Porosity could be elevated from the increased w:c ratios causing the salts to remain free and not bind to the cement matrix. Upon inspection of each sample after testing, an oxide film could be seen on some samples and de-cementation could be seen on the exposed surface. The oxide film is due to the corrosion of the graphite in the saltwater. Free ions travel through the solution and coalesce on the concrete. De-cementation is due to the salt attack on the concrete surface.

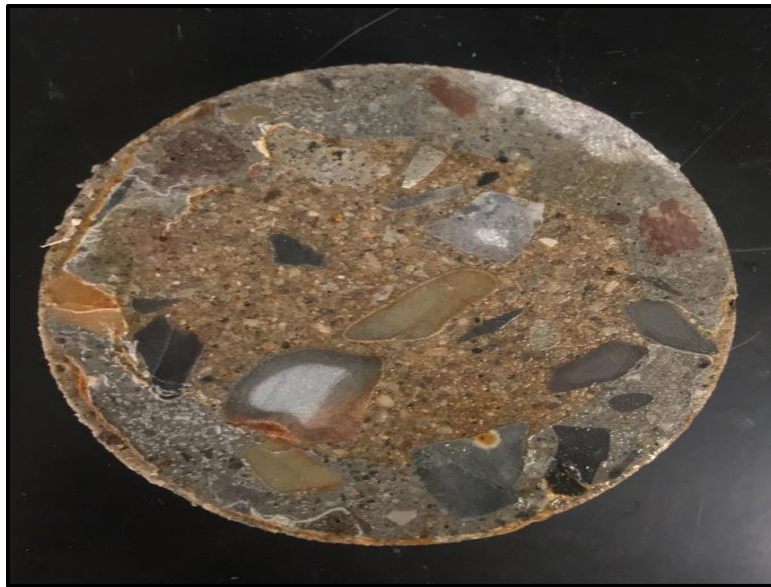


Figure 27 - Typical Rust Film Development and De-cementation of Exposure Surface

Disks with the 4 – 25:75 admixture ratio experienced equilibrium at different rates. Run 2 reached equilibrium after approximately 20 hours and run 1 reached it at approximately 60 hours. The different rates to equilibrium caused different concentration gradients to occur, see Figure 28 below. A wide sample standard deviation of flux and diffusion coefficient can be seen between the samples in Table 11. The wide range indicates that the average may not have been accurately represented. Data for the development of the concentration vs time curves can be seen in Appendix 6.4.1.

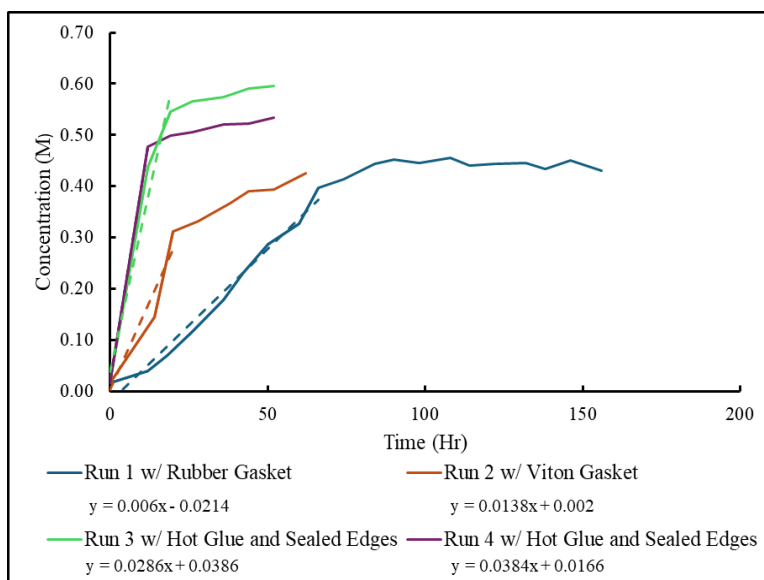


Figure 28 - Anolyte Concentration vs Time 4 - 25:75

Table 11 - Flux, Diffusion Coefficient, and Initial Catholyte Concentration 4 - 25:75

	DC/DT	J	D	Catholyte C_0
	M/hr	M/cm ² Hr (M/in ² hr)	cm ² /hr (in ² /hr)	M
Run 1	0.006	1.89e-4 (1.22e-3)	0.92e-6 (2.33e-6)	0.91
Run 2	0.0138	4.36e-4 (2.81e-3)	1.95e-6 (4.94e-6)	0.99
Run 3	0.0286	9.03e-4 (5.82e-3)	4.07e-6 (10.3e-6)	0.98
Run 4	0.0384	12.1e-4 (7.82e-3)	5.21e-6 (13.2e-6)	1.03
Average'	0.0099	3.12e-4 (2.01e-3)	1.43e-6 (3.64e-6)	0.95
SD'	0.0055	1.74e-4 (1.12e-3)	0.73e-6 (1.84e-6)	0.06

' Run 3 and 4 omitted from statistical analysis due to short circuiting in test

Disks with the 4 – 50:50 ratio diffused to equilibrium at similar rates, see Figure 29 below. This allowed concentration gradients and diffusion coefficients to display a narrower sample standard deviation range. With a narrower range, the averages for flux and diffusion coefficient could be better represented, see Table 12. It is important to note that the initial catholyte concentration between runs 2 and 4 had a large range for sample standard deviation. This indicates that initial catholyte concentration does play a role in the determination of diffusion coefficients. Different initial catholyte concentration between runs can occur due to insufficient mixing of saltwater. Data for the development of the concentration vs time curve can be seen in Appendix 6.4.2.

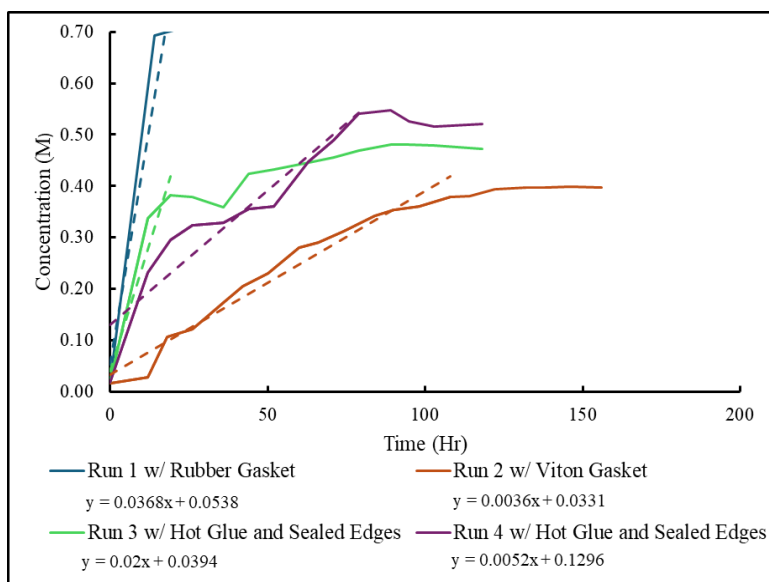


Figure 29 - Anolyte Concentration vs Time 4 - 50:50

Table 12 - Flux, Diffusion Coefficient, and Initial Catholyte Concentration 4 - 50:50

	DC/DT	J	D	Catholyte C_0
	M/hr	M/cm ² Hr (M/in ² hr)	cm ² /hr (in ² /hr)	M
Run 1	0.0368	11.6e-4 (7.49e-3)	5.04e-6 (12.7e-6)	1.02
Run 2	0.0036	1.13e-4 (0.73e-3)	0.71e-6 (1.80e-6)	0.71
Run 3	0.0200	6.32e-4 (4.07e-3)	2.88e-6 (7.31e-6)	0.97
Run 4	0.0052	1.64e-4 (1.06e-3)	0.72e-6 (1.83e-6)	1.01
Average'	0.0044	1.39e-4 (0.90e-3)	0.71e-6 (1.81e-6)	0.86
SD'	0.0011	0.36e-4 (0.23e-3)	0.007e-6 (0.02e-6)	0.21

'Run 1 and 3 omitted from statistical analysis due to short circuiting in test

Disks with the 4 – 75:25 ratio depicted dissimilar concentration gradients between each run, see Figure 30. Different initial catholyte concentrations also influenced the determination of diffusion coefficients. Overall, there is a wide range for the sample standard deviation of the flux and diffusion coefficient would indicate potential misrepresentation. Data for the development of the concentration vs time curves can be seen in appendix 6.4.3.

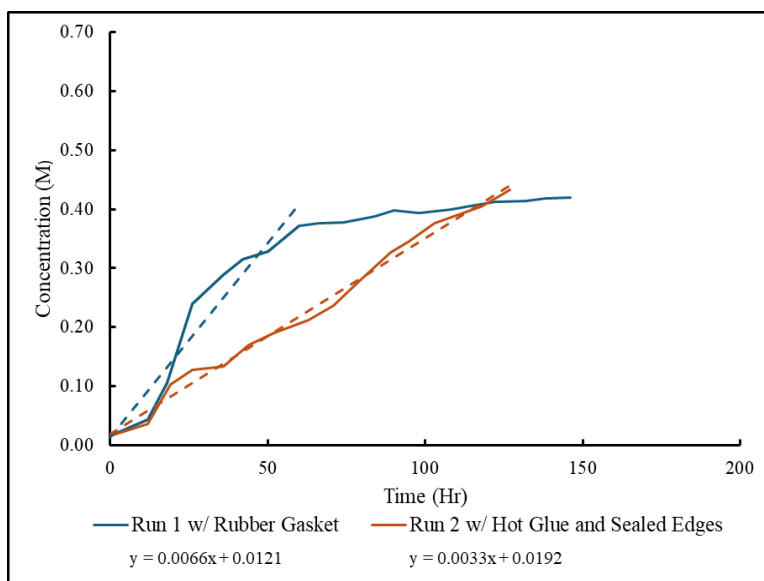


Figure 30 - Anolyte Concentration vs Time 4 - 75:25

Table 13 - Flux, Diffusion Coefficient, and Initial Catholyte Concentration 4 - 75:25

	DC/DT M/hr	J M/cm ² Hr (M/in ² hr)	D cm ² /hr (in ² /hr)	Catholyte C ₀ M
Run 1	0.0066	2.01e-4 (1.34e-3)	1.20e-6 (3.04e-6)	0.77
Run 2	0.0033	1.04e-4 (0.67e-3)	0.47e-6 (1.14e-6)	1.03
Average	0.0050	1.56e-4 (1.01e-3)	0.82e-6 (2.08e-6)	0.90
SD	0.0023	0.73e-4 (0.48e-3)	0.52e-6 (1.35e-6)	0.18

Testing of the 8 – 25:75 disks produced four runs. Each run has a similar change in concentration gradients. The steeper nature of the curves depicted in Figure 31 indicates that diffusion occurs at faster rates. Both flux and diffusion coefficient are large. The main reason sample standard deviation is wide for the diffusion coefficients is due to the wide deviation from the initial catholyte concentration. Data for the development of the concentration vs time curves can be seen in Appendix 6.4.4.

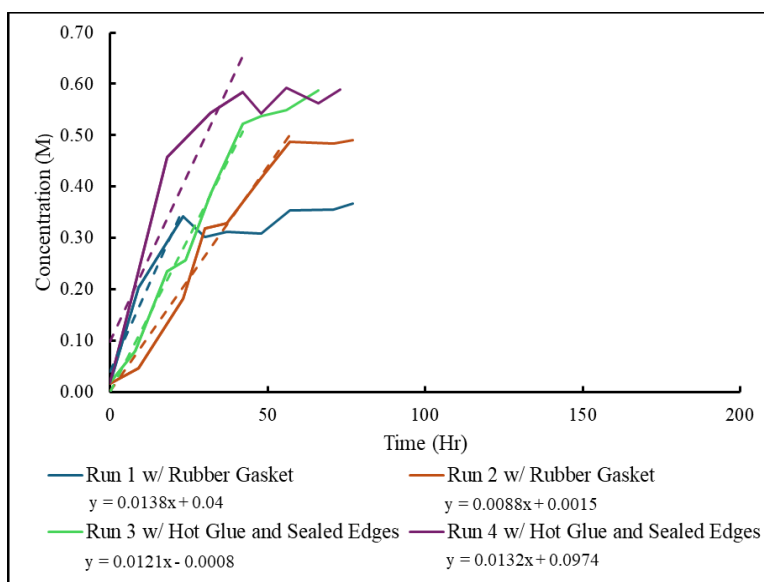


Figure 31 - Anolyte Concentration vs Time 8 - 25:75

Table 14 - Flux, Diffusion Coefficient, and Initial Catholyte Concentration 8 - 25:75

	DC/DT	J	D	Catholyte C_0
	M/hr	M/cm ² Hr (M/in ² hr)	cm ² /hr (in ² /hr)	M
Run 1	0.0138	4.35e-4 (2.81e-3)	3.16e-6 (8.02e-6)	0.61
Run 2	0.0088	2.78e-4 (1.79e-3)	1.20e-6 (3.06e-6)	1.02
Run 3	0.0121	3.82e-4 (2.46e-3)	1.69e-6 (4.29e-6)	1.00
Run 4	0.0132	4.17e-4 (2.68e-3)	1.88e-6 (4.78e-6)	0.98
Average	0.0120	3.78e-4 (2.44e-3)	1.98e-6 (5.04e-6)	0.90
SD	0.0022	0.71e-4 (0.45e-3)	0.83e-6 (2.12e-6)	0.20

Disks with the 8 – 50:50 ratio showed similar concentration gradients. However, run 1 showed salt binding. Salt binding caused contrasting times for equilibrium to occur. After 75 hours free chlorides were able to pass through the concrete and change the concentration of the anolyte tank. The narrow sample standard deviation for flux and diffusion coefficient indicated that the average was well represented. Data for the development of concentration vs time curves can be seen in Appendix 6.4.5.

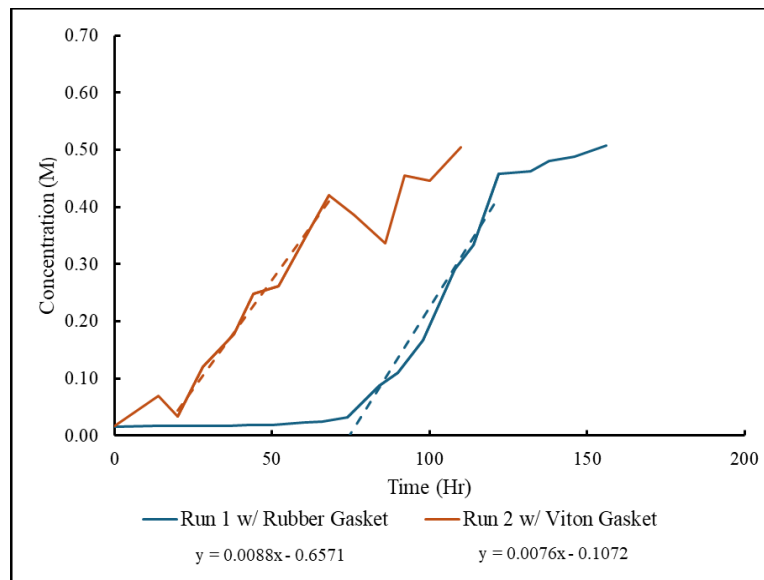


Figure 32 - Anolyte Concentration vs Time 8 - 50:50

Table 15 - Flux, Diffusion Coefficient, and Initial Catholyte Concentration 8 - 50:50

	DC/DT M/hr	J M/cm ² Hr (M/in ² hr)	D cm ² /hr (in ² /hr)	Catholyte C ₀ M
Run 1	0.0088	2.78e-4 (1.79e-3)	1.56e-6 (3.95e-6)	0.79
Run 2	0.0076	2.40e-4 (1.55e-3)	0.92e-6 (2.52e-6)	1.07
Average	0.0082	2.59e-4 (1.67e-3)	1.27e-6 (3.23e-6)	0.93
SD	0.0008	0.27e-4 (0.17e-3)	0.40e-6 (1.01e-6)	0.20

Disks with the 8 – 75:25 ratio showed dissimilar concentration gradients. Due to the difference of concentration gradients, a wide sample standard deviation could be depicted for the averages of flux and diffusion coefficients. Wide standard deviation could indicate misrepresentation of those values. Data for the development of concentration vs time curves can be seen in Appendix 6.4.6.

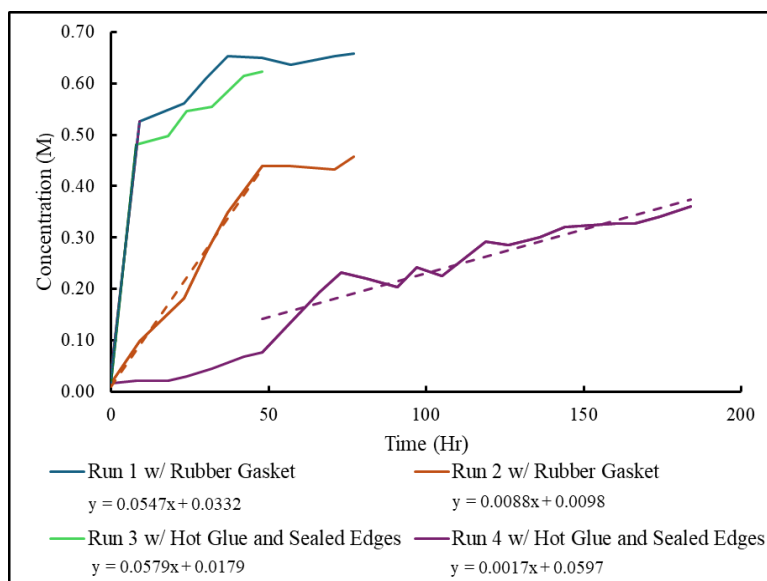


Figure 33 - Anolyte Concentration vs Time 8 - 75:25

Table 16 - Flux, Diffusion Coefficient, and Initial Catholyte Concentration 8 - 75:25

	DC/DT	J	D	Catholyte C ₀
	M/hr	M/cm ² Hr (M/in ² hr)	cm ² /hr (in ² /hr)	M
Run 1	0.0547	17.2e-4 (11.1e-3)	8.78e-6 (22.3e-6)	0.87
Run 2	0.0088	2.78e-4 (1.79e-3)	1.20e-6 (3.06e-6)	1.02
Run 3	0.0579	18.2e-4 (11.7e-3)	8.25e-6 (20.9e-6)	0.98
Run 4	0.0017	0.54e-4 (0.35e-3)	0.24e-6 (0.61e-6)	0.99
Average'	0.0053	1.65e-4 (1.06e-3)	0.72e-6 (1.83e-6)	1.005
SD'	0.0050	1.59e-4 (1.02e-3)	0.68e-6 (1.73e-6)	0.02

'Run 1 and 3 omitted from statistical analysis due to short circuiting in test

Control samples displayed the shallowest concentration vs time curves in testing. The shallowness correlates to slow diffusion rates. However, different concentration gradient change could be seen between the runs. A wide sample standard deviation for the flux and diffusion coefficient could indicate misrepresentation of the true values. Data for the development of concentration vs time curves can be seen in Appendix 6.4.7.

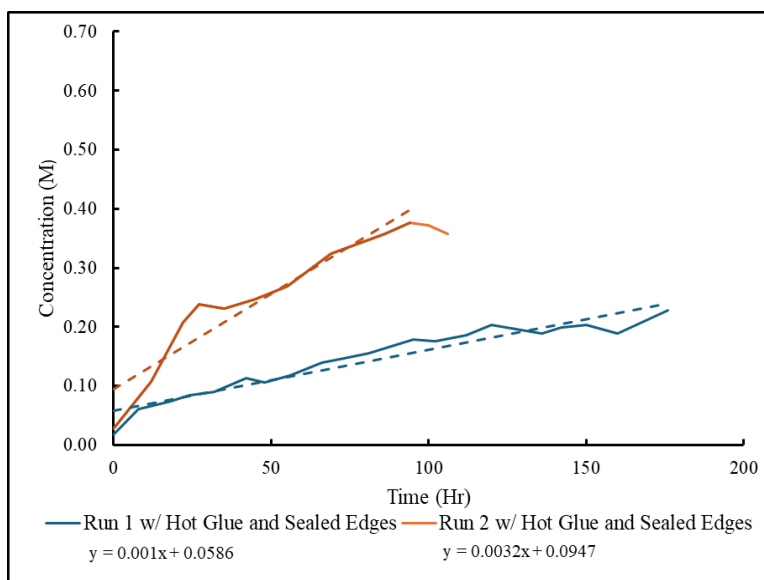


Figure 34 – Anolyte Concentration vs Time Control

Table 17 - Flux, Diffusion Coefficient, Initial Catholyte Concentration Control

	DC/DT M/hr	J M/cm ² Hr (M/in ² hr)	D cm ² /hr (in ² /hr)	Catholyte C ₀ M
Run 1	0.0010	0.32e-4 (0.20e-3)	0.14e-6 (0.35e-6)	1.02
Run 2	0.0032	1.01e-4 (0.65e-3)	0.45 e-6 (1.14e-6)	0.99
Average	0.0021	0.63e-4 (0.42e-3)	0.29e-6 (0.75e-6)	1.01
SD	0.0016	0.49e-4 (0.32e-3)	0.22e-6 (0.56e-6)	0.02

Overall, the control sample had the slowest diffusion of contaminant chloride, this was indicated by the smallest diffusion coefficient and smallest flux. Mixtures with elevated portions of bentonite displayed the fastest diffusion rates due to higher flux and diffusion coefficients. This can relate to the high w:c ratios that were developed in mixing which could influence porosity size. Reduced diffusion rates can be seen in the samples with increased biochar content. Samples with more biochar were 2-3 times faster than the control. Samples with more bentonite were 5-7 times faster than the control and twice as fast as the biochar rich samples.

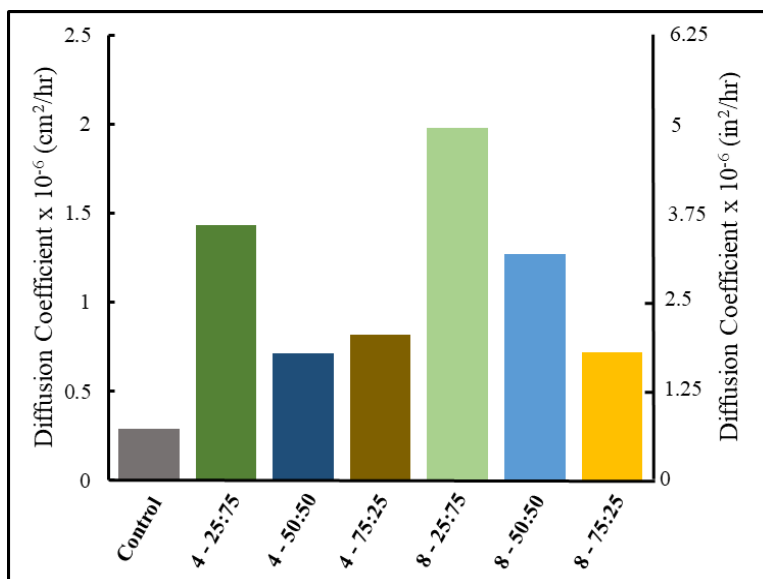


Figure 35 - Diffusion Coefficient Batch Comparison

Table 18 - Average Flux, Diffusion Coefficient, and Initial Catholyte Concentration Batch Comparison

	DC/DT	J	D	C ₀
	M/hr	M/cm ² Hr (M/in ² hr)	cm ² /hr (in ² /hr)	M
4 - 25:75	0.0099	3.12e-4 (2.01e-3)	1.43e-6 (3.64e-6)	0.95
4 - 50:50	0.0044	1.39e-4 (0.90e-3)	0.71e-6 (1.81e-6)	0.86
4 - 75:25	0.0050	1.56e-4 (1.01e-3)	0.82e-6 (2.08e-6)	0.90
8 - 25:75	0.0120	3.78e-4 (2.44e-3)	1.98e-6 (5.04e-6)	0.90
8 - 50:50	0.0082	2.59e-4 (1.67e-3)	1.27e-6 (3.23e-6)	0.93
8 - 75:25	0.0053	1.65e-4 (1.06e-3)	0.72e-6 (1.83e-6)	1.01
Control	0.0021	0.63e-4 (0.42e-3)	0.29e-6 (0.75e-6)	1.01

4.4 Strength Test and Density

In the compressive strength testing, each mixture was evaluated in triplicate. Triplicate analysis allowed for determination of a representative average compressive strength. Overall, the control sample had the largest average compression resistance available. Reduction of strength occurred for both the 4% by weight and 8% by weight samples. In the 4% by weight samples there was approximately 65% strength loss. In the 8% by weight samples strength loss was 75-95%. No trend was observed between the different ratios for the 4% by weight additions but a positive trend could be observed for the 8% by weight additions. The positive trend was an increase in strength with increased biochar addition. Example calculations and data for the development of the 28-day average compressive strength plot can be seen in Appendix 6.5.1.

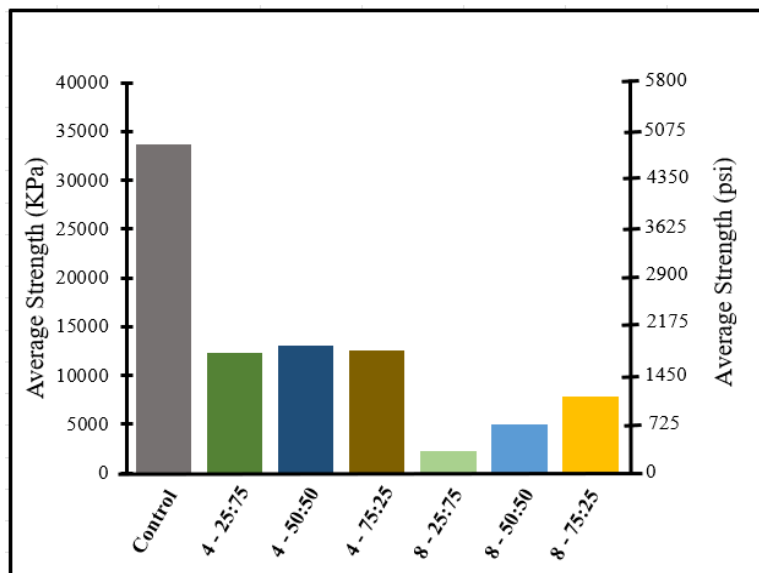


Figure 36 - Average 28 Day Compressive Strength

Table 19 – Average Peak Load and 28 Day Compressive Strength

	Peak Load KN (lbf)	Strength kPa (psi)
Control	272.4 (61,250)	33,620 (4,880)
4-25:75	99.7 (22,420)	12,310 (1,790)
4-50:50	105.6 (23,730)	13,030 (1,890)
4-75:25	101.3 (22,775)	12,500 (1,810)
8-25:75	18.4 (4,130)	2,270 (329)
8-50:50	40.8 (9,170)	5,030 (729)
8-75:25	63.8 (14,340)	7,870 (1,140)

- X-Sctn Area of test specimens 8.1×10^{-3} (12.56) m² (in²)

Only one test from each ratio was tested for bending strength. Similar trends were observed between the compression strength analysis and the bending strength analysis. Ultimately, the control sample had the highest resistance to bending. Strength decreased for both the 4% and 8% by weight additions. In the 4% sample strength loss compared to the control was 10-25%. In the 8% samples strength loss was 25-75% compared to the control. Both the 4% and 8% by weight additions portrayed the trend of increased strength with increased implementation of biochar. However, the 8% by weight addition had a greater decrease in available strength when compared to the 4% by weight addition. Example calculations and data for the development of the 28-day bending strength plot can be seen in Appendix 6.5.2.

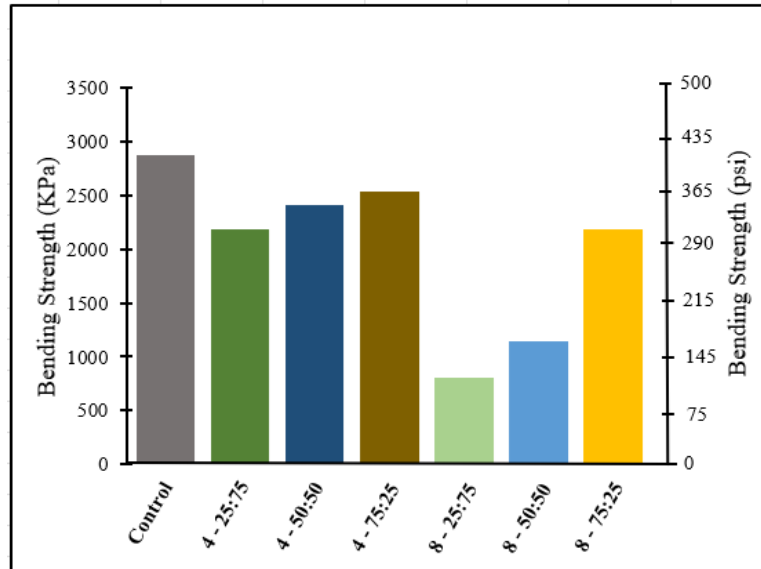


Figure 37 – 28 Day Bending Strength

Table 20 - Peak Load, Maximum Moment, And 28 Day Bending Strength

	Peak Load kN (lbf)	Moment kN-m (lbf-in)	Bending Strength kPa (psi)
Control	22.2 (5,000)	1.69 (15,000)	2,870 (417)
4-25:75	16.9 (3,800)	1.29 (11,400)	2,180 (317)
4-50:50	18.7 (4,200)	1.42 (12,600)	2,410 (350)
4-75:25	19.6 (4,400)	1.49 (13,200)	2,530 (367)
8-25:75	6.2 (1,400)	0.47 (4,200)	800 (117)
8-50:50	8.9 (2,000)	0.68 (6,000)	1,150 (166)
8-75:25	16.9 (3,800)	1.29 (11,400)	2,180 (317)

Prior to the testing of the cylinders, each cylinder was weighed. The weight could be coupled with the known volume of the sample to derive different densities. Overall, the control sample had the highest density. Each of the samples with the 4% and 8% by weight additions showed minimal decrease in density. Density can decrease because the specific gravity of biochar and bentonite is less than that of water in concrete. Example calculations and data for the development of the density plot can be seen in Appendix 6.5.3.

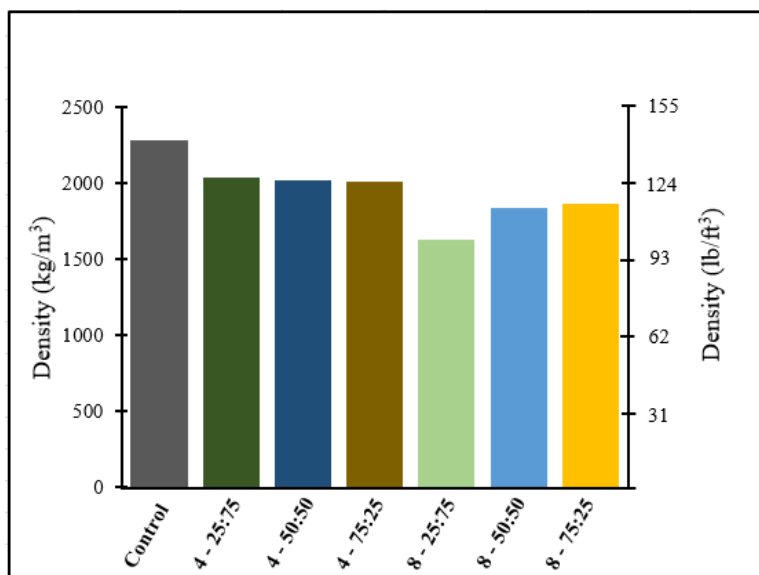


Figure 38 - Average Density

Table 21 - Weight and Density

	Weight kg (lbs)	Density kg/m ³ (lbs/ft ³)
Control	3.4 (7.6)	2287 (143)
4-25:75	3.4 (7.4)	2035 (127)
4-50:50	3.3 (7.3)	2017 (126)
4-75:25	3.3 (7.3)	2012 (126)
8-25:75	2.7 (6.0)	1633 (102)
8-50:50	3.0 (6.7)	1840 (115)
8-75:25	3.1 (6.8)	1862 (116)

5.0 Conclusion

Overall, the control sample excelled in each testing scenario. It had less susceptibility of corrosion risk in open circuit potential testing, slower rates of diffusion in the forced migration testing, and higher resistance characteristics in strength testing. A common trend through each test was 4% by weight additions of biochar and bentonite had less of an impact on corrosion prevention suitability than 8% by weight additions. Another common trend observed was suitability characteristics improved with increased amounts of biochar implementation.

5.1 Limitations

The performance of each mixing ratio is likely influenced by the high w:c ratios created during mixing. Higher w:c ratios are attributed to the water retention of biochar and bentonite. Elevated water retention decreased fluidity of the concrete mixes. To maintain a consistent fluidity index water was continually added until a desired slump was achieved. Excess water caused overhydration which could cause larger porosity within the mixes and decreased strength. Larger porosity can influence suitability of the open circuit potential and forced migration tests. Ultimately, the excellent performance from the control samples could be attributed to the lowest w:c between each mix.

Additionally, each mix design called for too little fine aggregate content and too much water content due to miscalculation of the modified correction factors. For the calculation of the modified fine aggregate, the weight of the original coarse aggregate was used instead of the original fine aggregate. Since modified fine aggregate weight was incorrect, the calculation of modified water weight was also incorrect. Correct modified weights for each control mix should have been as follows:

Table 22 - Corrected Modification Factors for Fine Aggregate and Water Weight in Mix 1

Used W_{FA}	Actual W_{FA}	Used W_{WA}	Actual W_{WA}
kg (lb)	kg (lb)	kg (lb)	kg (lb)
21.0 (46.4)	30.4 (67.0)	14.6 (32.2)	5.3 (11.7)

Table 23 - Corrected Modification Factor for Fine Aggregate and Water Weight in Mix 2

Used W_{FA}	Actual W_{FA}	Used W_{WA}	Actual W_{WA}
kg (lb)	kg (lb)	kg (lb)	kg (lb)
24.0 (52.8)	34.5 (76.1)	16.6 (36.7)	6.1 (13.4)

5.2 Recommendations

Based on the performance of the bentonite rich samples in this research, bentonite should be omitted from further work. Even with an influence of high w:c, increased bentonite mixtures exhibited decreased suitability of corrosion prevention when compared to elevated addition of biochar. Mixing with bentonite required more water to overcome the water retention characteristics. With bentonite removed, water retention capacity could decrease. Any further retention from the biochar could be overcome with the use of a plasticizer to increase mixing fluidity.

5.3 Future Work

In addition to the future work designated above, further research could include, a long-term study of suitability under normal exposure conditions instead of accelerated testing, determination of the adsorptive capacity of the biochar in the concrete and at what point that capacity is reached in the life of concrete, characterization of which biochar type would be most suitable for contaminant adsorbing, and a life cycle assessment.

6.0 Appendix

6.1 ACI 211 Design Tables

Table 6.3.1

Table 6.3.1 – Recommended slumps for various types of construction*

Types of construction	Slump, in.	
	Maximum+	Minimum
Reinforced foundation walls and footings	3	1
Plain footings, caissons, and substructure walls	3	1
Beams and reinforced walls	4	1
Building columns	4	1
Pavements and slabs	3	1
Mass concrete	2	1

Table 6.3.3

ACI COMMITTEE REPORT

Table 6.3.3 — Approximate mixing water and air content requirements for different slumps and nominal maximum sizes of aggregates

Water, lb/yd ³ of concrete for indicated nominal maximum sizes of aggregate								
Slump, in.	⅜ in.*	½ in.*	¾ in.*	1 in.*	1-½ in.*	2 in.* [†]	3 in. ^{†‡}	6 in. ^{†‡}
Non-air-entrained concrete								
1 to 2	350	335	315	300	275	260	220	190
3 to 4	385	365	340	325	300	285	245	210
6 to 7	410	385	360	340	315	300	270	—
More than 7*	—	—	—	—	—	—	—	—
Approximate amount of entrapped air in non-air-entrained concrete, percent	3	2.5	2	1.5	1	0.5	0.3	0.2
Air-entrained concrete								
1 to 2	305	295	280	270	250	240	205	180
3 to 4	340	325	305	295	275	265	225	200
6 to 7	365	345	325	310	290	280	260	—
More than 7*	—	—	—	—	—	—	—	—
Recommended averages [†] total air content, percent for level of exposure:								
Mild exposure	4.5	4.0	3.5	3.0	2.5	2.0	1.5*** ^{††}	1.0** ^{††}
Moderate exposure	6.0	5.5	5.0	4.5	4.5	4.0	3.5*** ^{††}	3.0** ^{††}
Severe exposure ^{††}	7.5	7.0	6.0	6.0	5.5	5.0	4.5*** ^{††}	4.0** ^{††}

Table 6.3.4b

Table 6.3.4(b) – Maximum permissible water-cement or water-cementitious materials ratios for concrete in severe exposures*

Type of structure	Structure wet continuously or frequently and exposed to freezing and thawing ⁺	Structure exposed to sea water or sulfates
Thin sections (railings, curbs, sills, ledges, ornamental work) and sections with less than 1 in. cover over steel	0.45	0.40+
All other structures	0.50	0.45+

Table 6.3.6

Table 6.3.6 – Volume of coarse aggregate per unit of volume of concrete

Nominal maximum size of aggregate, in.	Volume of oven-dry-rodded coarse aggregate* per unit volume of concrete for different fineness moduli of fine aggregate ⁺			
	2.40	2.60	2.80	3.00
3/8	0.50	0.48	0.46	0.44
1/2	0.59	0.57	0.55	0.53
3/4	0.66	0.64	0.62	0.60
1	0.71	0.69	0.67	0.65
1 1/2	0.75	0.73	0.71	0.69
2	0.78	0.76	0.74	0.72
3	0.82	0.80	0.78	0.76
6	0.87	0.85	0.83	0.81

6.2 Mix Design Calculations

6.2.1 Mix 1 Design Calculations

Volume of Samples per Batch

- 3 – 12” x 12” x 4” slabs = 1cf
- 1 – 4” diameter 8” cylinder = 0.05cf
= 1.05cf

Design Assumptions

- 3-4” slump for reinforced structures (6.3.1)
- Severe air exposure 6% (6.3.3)
 - Concrete is heavily exposed to contaminants
- Use of ¾” aggregate
- Weight of mixing Water (6.3.3)
 - 305 lb/cy
- Fineness moduli = 2.7 (6.3.6)
- Coarse aggregate unit weight = 100pcf
- Volume of fines: coarse = 0.63
- Water unit weight = 62.4 lb/cf
- Specific Gravity
 - Cement = 3.15
 - Fine Aggregate = 2.68
 - Coarse Aggregate = 2.75
- Absorption capacity and moisture content of fines and coarse
 - Fines
 - ABS = 1.2%
 - MC = 1.019
 - Coarse
 - ABS = 0.6%
 - MC = 1
- Biochar is fine aggregate replacement
- Bentonite is cement replacement
- W:C = 0.45 (6.3.4b)

Calculations

$$\begin{aligned} \text{Water weight} &= (\text{volume required})(\text{weight of mixing water}) \\ &= (1.05\text{cf})(1\text{cy}/27\text{cf})(305\text{lb/cy}) \\ &= 11.92 \text{ lb} \end{aligned}$$

$$\begin{aligned} \text{Cement Weight} &= \text{water weight}/w:c \\ &= 11.92 \text{ lb}/0.45 \\ &= 26.50 \text{ lb} \end{aligned}$$

$$\begin{aligned} \text{Fine aggregate weight} &= (\text{coarse unit weight})(\text{fines: coarse})(\text{volume required}) \\ &= (100\text{pcf})(0.63)(1.05\text{cf}) \\ &= 66.51 \text{ lb} \end{aligned}$$

$$\begin{aligned} \text{Air volume} &= (6\%)(\text{volume required}) \\ &= (.06)(1.05\text{cf}) \\ &= 0.06\text{cf} \end{aligned}$$

$$\begin{aligned} \text{Water volume} &= \text{water weight} / (\text{SPG})(\text{water unit weight}) \\ &= 11.92 \text{ lb} / (1)(62.4\text{pcf}) \\ &= 0.19\text{cf} \end{aligned}$$

$$\begin{aligned} \text{Cement volume} &= \text{cement weight} / (\text{SPG})(\text{water unit weight}) \\ &= 26.50 \text{ lb} / (3.15)(62.4\text{pcf}) \\ &= 0.14\text{cf} \end{aligned}$$

$$\begin{aligned} \text{Fine aggregate volume} &= \text{fine weight} / (\text{SPG})(\text{water unit weight}) \\ &= 66.51 \text{ lb} / (2.68)(62.4\text{pcf}) \\ &= 0.40\text{cf} \end{aligned}$$

$$\begin{aligned} \text{Coarse volume} &= \text{volume required} - \text{sum}(\text{component volumes}) \\ &= 1.05 \text{ cf} - (.4+.14+.19+.06)\text{cf} \\ &= .27\text{cf} \end{aligned}$$

$$\begin{aligned} \text{Coarse weight} &= (\text{water unit weight})(\text{SPG})(\text{coarse volume}) \\ &= (62.4\text{pcf})(.27\text{cf})(2.75) \\ &= 46.1 \text{ lb} \end{aligned}$$

Modifications

$$\begin{aligned} \text{Modified coarse weight} &= (\text{Coarse weight})((1)(MC)/(1+ABS)) \\ &= (46.1 \text{ lb})((1)(1)/(1+.006)) \\ &= 45.8 \text{ lb} \end{aligned}$$

$$\begin{aligned} \text{Modified fine weight} &= (\text{fine weight})((1)(MC)/(1+ABS)) \\ &= (66.51 \text{ lb})((1)(1.019)/(1+.012)) \\ &= 67 \text{ lb} \end{aligned}$$

*In original calculation, coarse weight was used yielding 46.4 lb. This was used in each mix.

$$\begin{aligned} \text{Modified water weight} &= \text{sum(original components)} - \text{cement weight} - \text{sum(modified aggregates)} \\ &= 151.04 \text{ lb} - 26.5 \text{ lb} - 45.8 \text{ lb} - 67.1 \text{ lb} \\ &= 11.74 \text{ lb} \end{aligned}$$

Biochar / Bentonite Additions

$$\begin{aligned} 4\% \text{ by weight addition} &= (.04)(\text{sum(components)}) \\ &= (.04)(151.04 \text{ lb}) \\ &= 6.04 \text{ lb} \end{aligned}$$

*Weight broken down further with different BC:B ratios

$$\begin{aligned} 8\% \text{ by weight addition} &= (.08)(\text{sum(components)}) \\ &= (.08)(151.04 \text{ lb}) \\ &= 12.1 \text{ lb} \end{aligned}$$

*weight broken down further with different BC:B ratios

6.2.2 Mix 2 Design Calculations

Volume of Samples per Batch

- 5 – 4” diameter 8” cylinder = 0.25cf
- 1 – 6” x 6” x 21” beam = 0.44cf
= 1.20cf

Design Assumptions

- 3-4” slump for reinforced structures (6.3.1)
- Severe air exposure 6% (6.3.3)
 - Concrete is heavily exposed to contaminants
- Use of ¾” aggregate
- Weight of mixing Water (6.3.3)
 - 305 lb/cy
- Fineness moduli = 2.7 (6.3.6)
- Coarse aggregate unit weight = 100pcf
- Volume of fines: coarse = 0.63
- Water unit weight = 62.4 lb/cf
- Specific Gravity
 - Cement = 3.15
 - Fine Aggregate = 2.68
 - Coarse Aggregate = 2.75
- Absorption capacity and moisture content of fines and coarse
 - Fines
 - ABS = 1.2%
 - MC = 1.019
 - Coarse
 - ABS = 0.6%
 - MC = 1
- Biochar is fine aggregate replacement
- Bentonite is cement replacement
- W:C = 0.45 (6.3.4b)

Calculations

$$\begin{aligned} \text{Water weight} &= (\text{volume required})(\text{weight of mixing water}) \\ &= (1.20\text{cf})(1\text{cy}/27\text{cf})(305\text{lb/cy}) \\ &= 13.56 \text{ lb} \end{aligned}$$

$$\begin{aligned} \text{Cement Weight} &= \text{water weight}/w:c \\ &= 13.56 \text{ lb}/0.45 \\ &= 30.12 \text{ lb} \end{aligned}$$

$$\begin{aligned} \text{Fine aggregate weight} &= (\text{coarse unit weight})(\text{fines: coarse})(\text{volume required}) \\ &= (100\text{pcf})(0.63)(1.20\text{cf}) \\ &= 75.6 \text{ lb} \end{aligned}$$

$$\begin{aligned} \text{Air volume} &= (6\%)(\text{volume required}) \\ &= (.06)(1.20\text{cf}) \\ &= 0.07\text{cf} \end{aligned}$$

$$\begin{aligned} \text{Water volume} &= \text{water weight} / (\text{SPG})(\text{water unit weight}) \\ &= 13.56 \text{ lb} / (1)(62.4\text{pcf}) \\ &= 0.22\text{cf} \end{aligned}$$

$$\begin{aligned} \text{Cement volume} &= \text{cement weight} / (\text{SPG})(\text{water unit weight}) \\ &= 30.12 \text{ lb} / (3.15)(62.4\text{pcf}) \\ &= 0.15\text{cf} \end{aligned}$$

$$\begin{aligned} \text{Fine aggregate volume} &= \text{fine weight} / (\text{SPG})(\text{water unit weight}) \\ &= 75.6 \text{ lb} / (2.68)(62.4\text{pcf}) \\ &= 0.45\text{cf} \end{aligned}$$

$$\begin{aligned} \text{Coarse volume} &= \text{volume required} - \text{sum}(\text{component volumes}) \\ &= 1.20 \text{ cf} - (.45+.15+.22+.07)\text{cf} \\ &= .30\text{cf} \end{aligned}$$

$$\begin{aligned} \text{Coarse weight} &= (\text{water unit weight})(\text{SPG})(\text{coarse volume}) \\ &= (62.4\text{pcf})(.30\text{cf})(2.75) \\ &= 52.4 \text{ lb} \end{aligned}$$

Modifications

$$\begin{aligned} \text{Modified coarse weight} &= (\text{Coarse weight})((1)(MC)/(1+ABS)) \\ &= (52.4 \text{ lb})((1)(1)/(1+.006)) \\ &= 52.1 \text{ lb} \end{aligned}$$

$$\begin{aligned} \text{Modified fine weight} &= (\text{fine weight})((1)(MC)/(1+ABS)) \\ &= (75.6 \text{ lb})((1)(1.019)/(1+.012)) \\ &= 76.12 \text{ lb} \end{aligned}$$

*In original calculation, coarse weight was used yielding 52.8 lb. This was used in each mix.

$$\begin{aligned} \text{Modified water weight} &= \text{sum(original components)} - \text{cement weight} - \text{sum(modified aggregates)} \\ &= 171.68 \text{ lb} - 30.12 \text{ lb} - 52.1 \text{ lb} - 76.12 \text{ lb} \\ &= 13.34 \text{ lb} \end{aligned}$$

Biochar / Bentonite Additions

$$\begin{aligned} 4\% \text{ by weight addition} &= (.04)(\text{sum(components)}) \\ &= (.04)(171.68 \text{ lb}) \\ &= 6.87 \text{ lb} \end{aligned}$$

*Weight broken down further with different BC:B ratios

$$\begin{aligned} 8\% \text{ by weight addition} &= (.08)(\text{sum(components)}) \\ &= (.08)(171.68 \text{ lb}) \\ &= 13.73 \text{ lb} \end{aligned}$$

*weight broken down further with different BC:B ratios

6.3 Open Circuit Potential Data

6.3.1 Electrical Potential Voltage for Samples in NaCl

Sequence in Cycle	Days	8 - 75/25	8 - 50/50	8 - 25/75	4 - 75/25	4 - 50/50	4 - 25/75	Control
c1 w3	11	-317	-208.2	-576	-281	-532	-283	-140
c1 d3	14	-208.3	-206.2	-478	-261.6	-521	-229.7	-134
c2 w4	18	-285.6	-255.4	-544	-239.3	-548	-242.8	-137.7
c2 d4	22	-117.8	-320	-483	-232.5	-519	-232.8	-186.9
c2 w3	25	-439	-496	-483	-204.8	-544	-442	-131.4
c2 d3	28	-447	-131.1	-148.9	-87.5	-72.2	-114.7	-47.2
c3 w4	32	-501	-139.9	-547	-117.5	-125.7	-541	-127.9
c3 d4	36	-487	-350.4	-494	-139.9	-139.7	-501	-143.8
c3 w3	39	-555	-437	-592	-123.8	-150.8	-543	-135.1
c3 d3	42	-517	-476	-547	-144.7	-155.1	-535	-16.6
c4 w4	46	-633	-566	-650	-138.9	-240.1	-548	-142.6
c4 d4	50	-534	-537	-557	-144.2	-157.9	-509	-153.6
c4 w3	53	-622	-573	-636	-133.9	-217.6	-535	-147.3
c4 d3	56	-556	-550	-582	-143.8	-421	-541	-155.5
c5 w4	60	-623	-585	-655	-140	-517	-569	-151.2
c5 d4	64	-577	-572	-581	-292.5	-521	-549	-145.5
c5 w3	67	-623	-608	-648	-382.7	-545	-570	-147
c5 d3	70	-563	-576	-553	-416	-512	-533	-138.8
c6 w4	74	-623	-618	-614	-442	-550	-572	-383
c6 d4	78	-574	-581	-570	-461	-537	-551	-385.4
c6 w3	81	-617	-607	-630	-475	-553	-589	-418
c6 d3	84	-578	-588	-586	-474	-567	-580	-391.7

6.3.2 Electrical Potential Voltage for Samples in Ca(OH)₂

Sequence in Cycle	Days	8 - 75/25	8 - 50/50	8 - 25/75	4 - 75/25	4 - 50/50	4 - 25/75	Control
c1 w3	11	-190.7	-151.5	-234.8	-183.2	-174.7	-163.4	-102.9
c1 d3	14	-56.3	-113.3	-136.8	-116.3	-129.3	-131.3	-47.9
c2 w4	18	-157.6	-143.6	-240.5	-125.4	-140.7	-144.8	-75.9
c2 d4	22	-12	-46.7	-107.7	-91	-97.3	-62.4	-61
c2 w3	25	-136.5	-122.6	-201	-101.2	-109.8	-138.2	-52.4
c2 d3	28	-6.5	-484	-512	-457	-537	-193.8	-123
c3 w4	32	-104.2	-520	-601	-190.1	-531	-506	-133.8
c3 d4	36	-25.9	-510	-496	-172	-516	-502	-97.2
c3 w3	39	-133.3	-557	-597	-149.7	-550	-519	-120.1
c3 d3	42	-36.6	-539	-532	-153.8	-529	-523	-123.8
c4 w4	46	-221.5	-598	-657	-238.4	-578	-548	-122.9
c4 d4	50	-43.5	-535	-538	-266.2	-526	-493	-59.9
c4 w3	53	-133.7	-598	-621	-410	-565	-522	-123.8
c4 d3	56	-539	-528	-542	-394.7	-518	-504	-52.9
c5 w4	60	-112.4	-572	-623	-420	-528	-496	-135.5
c5 d4	64	-64.7	-523	-510	-437	-518	-496	-75.8
c5 w3	67	-122.1	-606	-632	-452	-550	-530	-107.8
c5 d3	70	-94.5	-523	-531	-434	-522	-445	-96.5
c6 w4	74	-167.1	-575	-594	-459	-538	-531	-191.8
c6 d4	78	-118	-513	-527	-456	-527	-509	-59.6
c6 w3	81	-310.3	-561	-577	-443	-536	-538	-109.7
c6 d3	84	-285.2	-524	-533	-456	-516	-511	-141.7

6.3.3 Electrical Potential Voltage for Samples in Na₂SO₄

Sequence in Cycle	Days	8 - 75/25	8 - 50/50	8 - 25/75	4 - 75/25	4 - 50/50	4 - 25/75	Control
c1 w3	11	-232.4	-164.0	-213.3	-158.2	-264.4	-232.4	-113.0
c1 d3	14	-184.6	-155.7	-174.9	-158.1	-233.2	-212.8	-126.0
c2 w4	18	-234.4	-172.1	-222.8	-133.2	-274.7	-163.9	-117.5
c2 d4	22	-192.0	-163.1	-255.4	-160.5	-265.8	-163.6	-103.9
c2 w3	25	-282.5	-176	-272.4	-160.3	-227.8	-165.7	-126.1
c2 d3	28	-224.8	-167.5	-194.2	-169.3	-178.1	-164.5	-123.4
c3 w4	32	-442.0	-169.7	-372.1	-160.1	-161.1	-155.4	-111.1
c3 d4	36	-436.0	-125.5	-262.9	-170.8	-166.8	-160.7	-101.4
c3 w3	39	-581	-184.6	-318.9	-159.8	-156	-154	-101.9
c3 d3	42	-528	-190.3	-247.3	-168.9	-162.2	-162	-114.8
c4 w4	46	-706.0	-618.0	-480.0	-163.6	-308.5	-342.6	-137.7
c4 d4	50	-549.0	-301.7	-470.0	-167.2	-205.2	-207.5	-116.5
c4 w3	53	-676	-474	-600	-164.2	-218.4	-141.1	-137.8
c4 d3	56	-545	-315.7	-506	-164.8	-201.7	-196.9	-113.8
c5 w4	60	-666.0	-461.0	-577.0	-162.8	-226.1	-175.0	-137.8
c5 d4	64	-566.0	-262.8	-533.0	-196.6	-184.7	-164.6	-120.5
c5 w3	67	-661	-256.7	-627	-168.3	-170.4	-167.8	-132.4
c5 d3	70	-591	-273.9	-567	-172.2	-163.5	-152	-126.1
c6 w4	74	-656.0	-289.8	-633.0	-165.8	-164.4	-156.5	-153.9
c6 d4	78	-599.0	-261.8	-533.0	-162.8	-155.8	-156.1	-151.9
c6 w3	81	-637	-252.6	-600	-163.8	-160.8	-154.8	-151.5
c6 d3	84	-601	-298.2	-535	-162	-155.4	-152.9	-147.7

6.4 Forced Migration Calculations and Data

$$D = \frac{J R T L}{V F C_0 Z}$$

J = concentration flux

R = Gas Constant = 8.3145 J / Mol K

T = Temperature = 22°C + 273 = 295 K

L = Disk Thickness = 2.5 cm or 1 in

Z = charge of species

F = Faradays Constant = 96500 coulomb / mol e⁻

C₀ = Initial Catholyte Concentration

V = Applied Voltage = 14.6 V

Example calculation

For run 1 of 8 – 50:50 test, all other runs from each mix have same procedure.

$$DC / DT = 0.0088 \text{ M/hr}$$

$$J = DC / DT / A$$

$$= 0.0088 \text{ M/hr} / 31.66 \text{ cm}^2 \text{ or } 0.0088 \text{ M/hr} / 4.91 \text{ in}^2$$

$$= 2.77\text{e-}4 \text{ M/cm}^2\text{hr} \text{ or } 1.79\text{e-}3 \text{ M/in}^2\text{hr}$$

$$C_0 = 0.79\text{M}$$

$$D = (2.77\text{e-}4)(8.3145)(295)(2.54) / (1)(96500)(0.79)(14.6)$$

$$= 1.56\text{e-}6 \text{ cm}^2\text{/hr} \text{ or } 3.95\text{e-}6 \text{ in}^2\text{hr}$$

6.4.1 4 – 25:75

Run 3 w/ Hot Glue and Sealed Edges			Run 4 w/ Hot Glue and Sealed Edges		
Time Hr	Conductivity mS	Concentration M	Time Hr	Conductivity mS	Concentration M
0	79.60	0.98	0	83.40	1.03
0	0.1598	0.02	0	0.0458	0.02
12	34.84	0.44	12	38.08	0.48
19	43.80	0.55	19	39.86	0.50
26	45.45	0.57	26	40.45	0.51
36	46.14	0.57	36	41.72	0.52
44	47.47	0.59	44	41.80	0.52
52	47.87	0.60	52	42.84	0.53

Run 2 w/ Viton Gasket		
Time Hr	Conductivity mS	Concentration M
0	80.50	0.99
0	0.0658	0.02
14	10.70	0.15
20	24.44	0.31
28	26.05	0.33
38	29.03	0.37
44	30.88	0.39
52	31.15	0.39
62	33.86	0.43

Top time zero indicates initial catholyte concentration.

Run 1 w/ Rubber Gasket		
Time	Conductivity	Concentration
Hr	mS	M
0	73.60	0.91
0	0.0172	0.02
12	1.886	0.04
18	4.460	0.07
26	8.27	0.12
36	13.37	0.18
42	17.71	0.23
50	22.33	0.29
60	25.64	0.33
66	31.54	0.40
74	32.87	0.41
84	35.35	0.44
90	35.97	0.45
98	35.46	0.45
108	36.36	0.46
114	35.03	0.44
122	35.40	0.44
132	35.42	0.44
138	34.49	0.43
146	35.94	0.45
156	34.21	0.43

Top time zero indicates initial catholyte concentration.

6.4.2 4 – 50:50

Run 3 w/ Hot Glue and Sealed Edges			Run 4 w/ Hot Glue and Sealed Edges		
Time Hr	Conductivity mS	Concentration M	Time Hr	Conductivity mS	Concentration M
0	79.10	0.97	0	82.10	1.01
0	0.1425	0.02	0	0.1852	0.02
12	26.59	0.34	12	17.83	0.23
19	30.23	0.38	19	23.09	0.30
26	29.99	0.38	26	25.45	0.32
36	28.29	0.36	36	25.82	0.33
44	33.66	0.42	44	28.11	0.36
52	34.43	0.43	52	28.53	0.36
63	35.52	0.45	63	35.69	0.45
71	36.36	0.46	71	39.12	0.49
79	37.37	0.47	79	43.43	0.54
89	38.35	0.48	89	43.99	0.55
95	38.38	0.48	95	42.13	0.53
103	38.22	0.48	103	41.31	0.52
118	37.74	0.47	118	41.74	0.52

Run 1 w/ Rubber Gasket		
Time Hr	Conductivity mS	Concentration M
0	82.70	1.02
0	0.0455	0.02
14	56.00	0.69
20	56.80	0.70

Top time zero indicates initial catholyte concentration.

Run 2 w/ Viton Gasket		
Time	Conductivity	Concentration
Hr	mS	M
0	57.00	0.71
0	0.0058	0.02
12	0.943	0.03
18	7.41	0.11
26	8.66	0.12
36	13.00	0.17
42	15.58	0.20
50	17.76	0.23
60	21.89	0.28
66	22.64	0.29
74	24.39	0.31
84	26.96	0.34
90	27.89	0.35
98	28.43	0.36
108	30.04	0.38
114	30.14	0.38
122	31.16	0.39
132	31.51	0.40
138	31.47	0.40
146	31.69	0.40
156	31.56	0.40

Top time zero indicates initial catholyte concentration.

6.4.3 4 – 75:25

Run 1 w/ Rubber Gasket			Run 2 w/ Hot Glue and Sealed Edges		
Time Hr	Conductivity mS	Concentration M	Time Hr	Conductivity mS	Concentration M
0	62.60	0.77	0	83.40	1.03
0	0.0078	0.02	0	0.0213	0.02
12	2.211	0.04	12	1.588	0.04
18	7.380	0.11	19	7.11	0.10
26	18.52	0.24	26	9.19	0.13
36	22.53	0.29	36	9.72	0.13
42	24.65	0.31	44	12.72	0.17
50	25.83	0.33	52	14.41	0.19
60	29.40	0.37	63	16.14	0.21
66	29.79	0.38	71	18.27	0.24
74	29.82	0.38	79	21.62	0.28
84	30.68	0.39	89	25.65	0.33
90	31.56	0.40	95	27.22	0.35
98	31.22	0.39	103	29.73	0.38
108	31.72	0.40	118	32.14	0.40
114	32.16	0.41	127	34.39	0.43
122	32.71	0.41			
132	32.89	0.41			
138	33.19	0.42			
146	33.33	0.42			

Top time zero indicates initial catholyte concentration.

6.4.4 8 – 25:75

Run 1 w/ Rubber Gasket			Run 2 w/ Rubber Gasket		
Time Hr	Conductivity mS	Concentration M	Time Hr	Conductivity mS	Concentration M
0	49.40	0.61	0	83.00	1.02
0	0.0478	0.02	0	0.0410	0.02
9	15.42	0.20	9	2.515	0.05
23	26.93	0.34	23	13.68	0.18
30	23.63	0.30	30	25.03	0.32
37	24.41	0.31	37	25.85	0.33
48	24.23	0.31	48	33.16	0.42
57	27.93	0.35	57	38.99	0.49
71	28.08	0.36	71	38.71	0.48
77	28.95	0.37	77	39.19	0.49

Run 3 w/ Hot Glue and Sealed Edges			Run 4 w/ Hot Glue and Sealed Edges		
Time Hr	Conductivity mS	Concentration M	Time Hr	Conductivity mS	Concentration M
0	81.3	1.00	0	79.9	0.98
0	0.096	0.02	0	0.1167	0.02
8	5.22	0.08	8	16.05	0.21
18	18.07	0.23	18	36.41	0.46
24	19.820	0.26	32	43.67	0.54
32	30.65	0.39	42	46.88	0.58
42	41.84	0.52	48	43.50	0.54
48	43.10	0.54	56	47.64	0.59
56	44.04	0.55	66	45.19	0.56
66	47.2	0.59	73	47.29	0.59

Top time zero indicates initial catholyte concentration.

6.4.5 8 – 50:50

Run 1 w/ Rubber Gasket			Run 2 w/ Viton Gasket		
Time Hr	Conductivity mS	Concentration M	Time Hr	Conductivity mS	Concentration M
0	63.70	0.79	0	87.20	1.07
0	0.0085	0.02	0	0.1521	0.02
12	0.0641	0.02	14	4.41	0.07
18	0.0792	0.02	20	1.481	0.03
26	0.1342	0.02	28	8.71	0.12
36	0.1494	0.02	38	13.32	0.18
42	0.1743	0.02	44	19.13	0.25
50	0.2602	0.02	52	20.25	0.26
60	0.5540	0.02	62	28.47	0.36
66	0.6750	0.02	68	33.38	0.42
74	1.282	0.03	76	30.61	0.39
84	5.88	0.09	86	26.55	0.34
90	7.76	0.11	92	36.24	0.45
98	12.46	0.17	100	35.58	0.45
108	22.81	0.29	110	40.36	0.50
114	26.21	0.33			
122	36.58	0.46			
132	36.88	0.46			
138	38.38	0.48			
146	39.01	0.49			
156	40.6	0.51			

Top time zero indicates initial catholyte concentration.

6.4.6 8 – 75:25

Run 1 w/ Rubber Gasket			Run 2 w/ Rubber Gasket		
Time Hr	Conductivity mS	Concentration M	Time Hr	Conductivity mS	Concentration M
0	70.20	0.87	0	82.60	1.02
0	1.424	0.03	0	0.0795	0.02
9	42.09	0.53	9	6.76	0.10
23	45.05	0.56	23	13.77	0.18
30	49.10	0.61	30	21.07	0.27
37	52.60	0.65	37	27.49	0.35
48	52.30	0.65	48	34.94	0.44
57	51.20	0.64	57	34.94	0.44
71	52.70	0.65	71	34.43	0.43
77	53.00	0.66	77	36.51	0.46

Run 3 w/ Hot Glue and Sealed Edges		
Time Hr	Conductivity mS	Concentration M
0	79.80	0.98
0	0.1597	0.02
8	38.42	0.48
18	39.76	0.50
24	43.76	0.55
32	44.52	0.55
42	49.47	0.61
48	50.09	0.62

Top time zero indicates initial catholyte concentration.

Run 4 w/ Hot Glue and Sealed Edges		
Time	Conductivity	Concentration
Hr	mS	M
0	81.5	0.99
0	0.0622	0.02
8	0.3986	0.02
18	0.4491	0.02
24	1.160	0.03
32	2.452	0.05
42	4.335	0.07
48	5.00	0.08
56	9.33	0.13
66	14.74	0.19
73	17.87	0.23
81	16.94	0.22
91	15.45	0.20
97	18.72	0.24
105	17.29	0.23
119	22.79	0.29
126	22.20	0.28
136	23.52	0.30
144	25.11	0.32
160	25.70	0.33
166	25.70	0.33
174	26.80	0.34
184	28.52	0.36

Top time zero indicates initial catholyte concentration.

6.4.7 Control

Run 1 w/ Hot Glue and Sealed Edges			Run 2 w/ Hot Glue and Sealed Edges		
Time Hr	Conductivity mS	Concentration M	Time Hr	Conductivity mS	Concentration M
0	83.10	1.02	0	80.90	0.99
0	0.1027	0.02	0	0.9990	0.03
8	3.669	0.06	12	7.57	0.11
18	4.786	0.07	22	15.88	0.21
24	5.62	0.08	27	18.42	0.24
32	6.13	0.09	35	17.76	0.23
42	8.01	0.11	45	19.12	0.25
48	7.43	0.11	55	20.88	0.27
56	8.46	0.12	69	25.46	0.32
66	10.16	0.14	86	28.20	0.36
73	10.85	0.15	94	29.83	0.38
81	11.49	0.16	100	29.44	0.37
95	13.51	0.18	106	28.23	0.36
102	13.27	0.18			
112	14.1	0.19			
120	15.55	0.20			
136	14.34	0.19			
142	15.15	0.20			
150	15.85	0.20			
160	16.78	0.19			
176	17.6	0.23			

Top time zero indicates initial catholyte concentration.

6.5 Strength and Density Calculations and Data

6.5.1 28 Day Compressive Strength

$$F_c' = F / A$$

F = peak load

A = cross sectional area

Example Calculation

For 1 control sample from mix 2, all other samples have similar procedure.

$$F = 279.3 \text{ kN or } 62790 \text{ lb}$$

$$A = 8.1 \times 10^{-3} \text{ m}^2 \text{ or } 12.56 \text{ in}^2$$

$$F_c' = 279.3 \text{ kN} / 8.1 \times 10^{-3} \text{ m}^2 \text{ or } 62790 \text{ lb} / 12.56 \text{ in}^2$$

$$= 34470 \text{ kPa or } 5000 \text{ psi}$$

	Peak Load KN (lbf)	Strength KPa (psi)		Peak Load KN (lbf)	Strength KPa (psi)
control	279.3 (62,790)	34,470 (5000)	8-25:75	17.8 (4,000)	2,200 (318)
	270.2 (60,750)	33,350 (4,840)		19.2 (4,320)	2,370 (344)
	267.8 (60,210)	33,050 (4,790)		18.1 (4,070)	2,230 (324)
	272.4 (61,250)	33,620 (4,880)		18.4 (4,130)	2,270 (329)
4-25:75	99.6 (22,400)	13,000 (1,780)	8-50:50	35.0 (7,870)	4,320 (627)
	91.1 (20,470)	11,240 (1,630)		44.0 (9,880)	5,420 (787)
	108.5 (24,390)	13,390 (1,940)		43.4 (9,750)	5,350 (776)
	99.7 (22,420)	12,310 (1,790)		40.8 (9,170)	5,030 (729)
4-50:50	99.1 (22,280)	12,230 (1,770)	8-75:25	63.9 (14,360)	7,880 (1,140)
	103.5 (23,260)	12,770 (1,850)		62.0 (13,940)	7,650 (1,110)
	114.1 (25,650)	14,080 (2,040)		65.4 (14,710)	8,080 (1,170)
	105.6 (23,730)	13,030 (1,890)		63.8 (14,340)	7,870 (1,140)
4-75:25	-	-			
	96.9 (21,790)	11,960 (1,730)			
	105.7 (23,760)	13,040 (1,890)			
	101.3 (22,775)	12,500 (1,810)			

6.5.2 28 Day Bending Strength

$$\text{Sigma}_b = MC / I$$

M = maximum applied moment

C = centroid of flexed shape

I = area moment of inertia

Example Calculation

For 1 control sample from mix 2, all other samples have similar procedure.

$$M = PL/6$$

$$P = 22.24 \text{ kN or } 5000 \text{ lb}$$

$$L = .457 \text{ m or } 18\text{in}$$

$$M = 1.69 \text{ kN-m or } 15000 \text{ lb-in}$$

$$C = 0.076 \text{ m or } 3 \text{ in}$$

$$I = bh^3 / 12$$

$$= (0.152 \text{ m})^4 / 12 \text{ or } (6 \text{ in})^4 / 12$$

$$= 4.49\text{e-}5\text{m}^4 \text{ or } 108 \text{ in}^4$$

$$\text{Sigma}_b = 2870 \text{ kPa or } 417\text{psi}$$

6.5.3 Density

$$\rho = m/v$$

m = mass

v = volume

Example Calculation

For 1 control sample from mix 2, all other samples have similar procedure.

M = 376 kg or 8.3 lb

V = Ah

A = cross sectional area

H = height

V = 1.65e-3m³ or 5.8e-2ft³

$\rho = 2285 \text{ kg / m}^3$ or 143 pcf

	Weight kg (lbs)	Density kg/m ³ (lbs/ft ³)		Weight kg (lbs)	Density kg/m ³ (lbs/ft ³)
Control	3.7 (8.3)	2285 (143)	8-25:75	2.7 (6.0)	1638 (102)
	3.1 (6.9)	2290 (143)		2.7 (6.0)	1627 (101)
	3.4 (7.6)	2287 (143)		2.7 (6.0)	1633 (102)
4-25:75	3.4 (7.4)	2034 (127)	8-50:50	3.0 (6.8)	1876 (117)
	3.4 (7.4)	2037 (127)		3.0 (6.6)	1803 (112)
	3.4 (7.4)	2035 (127)		3.0 (6.7)	1840 (115)
4-50:50	3.3 (7.4)	2023 (126)	8-75:25	3.1 (6.8)	1859 (116)
	3.3 (7.3)	2010 (125)		3.1 (6.8)	1865 (116)
	3.3 (7.3)	2017 (126)		3.1 (6.8)	1862 (116)
4-75:25	3.3 (7.3)	2020 (126)			
	3.3 (7.3)	2003 (125)			
	3.3 (7.3)	2012 (126)			

7.0 Resources

- [1] Bye, G. C. *Portland Cement: Composition, Production and Properties*. Pergamon Press, NY, 1983.
- [2] Dynamic Concrete Pumping, “What are concrete aggregates?: Concrete aggregate types,” Dynamic Concrete Pumping, <https://www.dcpu1.com/blog/the-role-of-aggregates-in-concrete/> (accessed Mar. 31, 2024).
- [3] Mehta and Monteiro. (1993) *Concrete Structure, Properties, and Materials*, Prentice-Hall, Inc., Englewood Cliffs, NJ
- [4] G. Hillhouse, “Why does concrete need reinforcement?,” *Practical Engineering*, <https://practical.engineering/blog/2018/8/1/why-does-concrete-need-reinforcement> (accessed Apr. 5, 2024).
- [5] Chemical admixtures, <https://www.cement.org/cement-concrete/concrete-materials/chemical-Admixtures> (accessed Apr. 6, 2024).
- [6] R. M. Andrew, “Global Co2 Emissions from cement production,” *Earth System Science Data*, <https://essd.copernicus.org/articles/10/195/2018/> (accessed Mar. 31, 2024).
- [7] N. Huft, “Fundamentals of Nucleation and Solidification.” Montana Technological University, Butte Montana, Feb. 2024
- [8] E. McCafferty, “Getting Started on the Basics,” in *Introduction to Corrosion Science*, New York, NY: Springer Science and Business Media, LLC, 2010, pp. 13–31
- [9] A. F. A. Fuhaid and A. Niaz, “Carbonation and corrosion problems in reinforced concrete structures,” *MDPI*, <https://www.mdpi.com/2075-5309/12/5/586> (accessed Apr. 5, 2024).
- [10] S. Ahmad, “Reinforcement corrosion in concrete structures, its monitoring and service life prediction—a review,” *Cement and Concrete Composites*, vol. 25, no. 4–5, pp. 459–471, May 2003. doi:10.1016/s0958-9465(02)00086-0
- [11] “Highway bridge inspections,” U.S. Department of Transportation, <https://www.transportation.gov/testimony/highway-bridge-inspections>. (accessed Jan. 18, 2024).
- [12] G. Scientific, “Understanding and monitoring corrosion in reinforced concrete,” Giatec Scientific Inc., <https://www.giatecscientific.com/education/understanding-concrete-corrosion/> (accessed Jan. 18, 2024).

- [13] N. Huft, "Chemical Reactions in Fusion Welding." Montana Technological University, Butte Montana , Jan. 2024
- [14] "Corrosion of Embedded Metals," Corrosion of Embedded Materials, <https://www.cement.org/learn/concrete-technology/durability/corrosion-of-embedded-materials> (accessed Apr. 6, 2024).
- [15] M. J. Graham, "Passivity of Iron," The Electrochemistry Society,
- [16] I. Mariani, "Evaluating concrete quality with electrical resistivity," Giatec Scientific Inc., <https://www.giatecscientific.com/education/evaluating-concrete-quality-with-electrical-resistivity> (accessed Apr. 6, 2024).
- [17] F. Tang, "Steel rebar coatings for concrete structures," STRUCTURE magazine, <https://www.structuremag.org> (accessed Apr. 7, 2024).
- [18] Uk, "Corrosion management with sacrificial anodes," Corrosion Management with Sacrificial Anodes, <https://gbr.sika.com/en/construction/concreterepair/media/news/2017/corrosion-management-with-sacrificial-anodes.html> (accessed Apr. 7, 2024).
- [19] S . Hong *et al.*, "Determination of impressed current efficiency during accelerated corrosion of Reinforcement," *Cement and Concrete Composites*, vol. 108, p. 103536, Apr. 2020. doi:10.1016/j.cemconcomp.2020.103536
- [20] Saukko, P. J., Siegel, J. A., & Houck, M. M. (Eds.). (2013). Identification and Comparison. In *Encyclopedia of Forensic Sciences* (2nd ed., Vol. 2, pp. 129–137). Academic Press.
- [21] Praveen, S., Jegan, J., Bhagavathi Pushpa, T., Gokulan, R., & Bulgariu, L. (2022). Biochar for removal of dyes in contaminated water: An overview. *Biochar*, 4(1). <https://doi.org/10.1007/s42773-022-00131-8>.
- [22] S. S. Senadheera *et al.*, "Application of biochar in concrete – a review," *Cement and Concrete Composites*, vol. 143, p. 105204, Oct. 2023. doi:10.1016/j.cemconcomp.2023.105204
- [23] J. Lombardo, "Keep Painting Roads Black," For Construction Pros, <https://www.forconstructionpros.com/asphalt/article/20971405/keep-painting-roads-black> (accessed Apr. 18, 2024).
- [24] ACI Committee 211, *Standard Practice for Selecting Proportions for Normal, Heavyweight, and Mass Concrete*. Detroit, MI: American Concrete Institute, 1997.
- [25] "Bentonite for drilling Wells," PetroNaft, <https://www.petronaftco.com/bentonite-for-drilling-wells/> (accessed Apr. 19, 2024).

- [26] M. Achyutha Kumar Reddy and V. C. Khed, “Bentonite clay modified concrete,” *Sand in Construction*, Aug. 2022. doi:10.5772/intechopen.103803
- [27] C143/C143M standard test method for slump of hydraulic-cement concrete, https://www.astm.org/c0143_c0143m-12.html (accessed Apr. 20, 2024).
- [28] “Standard specification for ready-mixed concrete,” C94/C94M, https://www.astm.org/c0094_c0094m-22a.html (accessed Apr. 21, 2024).
- [29] “ASTM C876-22b Standard Test Method for Corrosion Potentials of Uncoated Reinforcing Steel in Concrete,” ASTM Compass,
- [30] H.-W. Song and V. Sarawathy, “Corrosion Monitoring of Reinforced Concrete Structures - A Review,” *International Journal of Electrochemical Sciences*, vol. 1, no. 28, Jan. 2007.
- [31] P. F. McGrath and R. D. Hooton, “Re-evaluation of the AASHTO T259 90-Day salt ponding test,” *Cement and Concrete Research*, vol. 29, no. 8, pp. 1239–1248, Aug. 1999. doi:10.1016/s0008-8846(99)00058-7
- [32] I. Sánchez, X. R. Nóvoa, G. de Vera, and M. A. Climent, “Microstructural modifications in Portland cement concrete due to forced Ionic migration tests. study by impedance spectroscopy,” *Cement and Concrete Research*, vol. 38, no. 7, pp. 1015–1025, Jul. 2008. doi:10.1016/j.cemconres.2008.03.012
- [33] M. McDunnigan, “Brine vs. conductivity,” Sciencing, <https://sciencing.com/facts-7774197-brine-vs-conductivity.html> (accessed Apr. 21, 2024).
- [34] *YSI Model 30 YSI Model 30M Handheld Conductivity and Temperature System Operations Manual*. Yellow Springs, Ohio: YSI, 2007.
- [35] “Standard test method for compressive strength of cylindrical concrete specimens,” C39/C39M, https://www.astm.org/c0039_c0039m-21.html (accessed Apr. 23, 2024).
- [36] “Standard test method for flexural strength of concrete (using simple beam with third-point loading),” C78, <https://www.astm.org/standards/c78> (accessed Apr. 23, 2024).